ANL-ART-129

Initial Argonne Sodium Draining Tests: Analysis of Test Results and Comparison with Water Draining Behavior

Nuclear Science and Engineering Division

ANL-ART-129

Initial Argonne Sodium Draining Tests: Analysis of Test Results and Comparison with Water Draining Behavior

prepared by
James J. Sienicki, David B. Chojnowski,* Ed Boron,* and Yoichi Momozaki
Nuclear Science and Engineering Division, Argonne National Laboratory
*Applied Materials Division, Argonne National Laboratory

May 21, 2018

ABSTRACT

Three initial sodium draining experiments have been carried out in which sodium was drained from a 0.46 m high 4.6 mm inner diameter vertical stainless steel tube wetted by the sodium representative of a sodium channel in a compact diffusion-bonded sodium-to-CO_2 heat exchanger. Prior to the startup of sodium testing, shakedown tests were conducted with water. In all three sodium experiments, the sodium drained efficiently from the channel. Sodium and water both drain efficiently from a 4.6 mm inner diameter vertical stainless steel tube. This is an important and good result for the design of compact diffusion-bonded heat exchanger sodium channels. Sodium drains more efficiently than water. This is also an important and good result for the design of compact diffusion-bonded heat exchanger sodium channels. The draining phenomena observed with sodium and water are significantly different. The draining of water involves an initial rapid slug draining phase followed by a linear rate draining phase followed by a slow draining phase involving draining of rivulets and drops. This behavior has previously been reported in the literature for viscous fluids. The draining of sodium involves an initial rapid slug draining phase but no discernable linear rate draining phase. There is a subsequent slow draining phase. However, unlike the slow draining phase with water that involves a number of rivulets and drops, the slow draining phase with sodium in two out of three sodium tests mainly involves a single discrete event in which a mass of sodium drains from the tube. This single discrete draining event encompasses most of the sodium mass remaining inside of the tube following the rapid slug draining phase. The existence of a single discrete draining event during the slow draining phase with sodium versus several rivulet and drop draining events with water is thought to simply reflect the fact that significantly lower mass fractions of liquid are left behind inside of the tube following the rapid slug draining phase with sodium relative to water. For the sodium tests, the progress of wetting of the stainless steel by sodium was monitored by means of the voltage drop across the tube outer diameter measured by pairs of opposing electrodes welded to the tube outer surface at three different elevations. The electrode data remarkably reveals phenomena during the sodium draining. The downward passage of the sodium slug trailing edge past each electrode was observed from which a mean slug trailing edge velocity could be determined. The subsequent slower increase in voltage drop suggests draining and thinning of a sodium film left behind upon the tube inner surface; wiggles in the voltage drop data are suggestive of the descent of waves on the film. It is thought that the draining sodium film collects as a mass likely near the lower end of the tube and detaches corresponding to the single discrete draining event observed in the load cell data. The minimum circular channel inner diameter for the draining of water and sodium without the formation of lenses that bridge the channel and may remain inside of the tube without draining is predicted with a correlation to be 2.2 mm. The highest priority for future sodium draining testing is to investigate other channel geometries such as a rectilinear channel or a semicircular channel.

Table of Contents

LIST OF FIGURES

LIST OF TABLES

1 Introduction

Argonne National Laboratory (Argonne) has been leading the development of Sodium-Cooled Fast Reactors (SFRs) and supercritical carbon dioxide (sCO_2) Brayton cycle power conversion for SFRs for the U.S. Department of Energy (DOE). Argonne has been leading the development of compact diffusion-bonded sodium-to-CO_2 heat exchangers for SFRs with sCO_2 Brayton cycle power conversion. There is an incentive to make the coolant channels on the sodium and CO_2 sides of the heat exchanger as small as possible to reduce the heat exchanger size and cost. However, there are practical limitations on how small the channels can be. In the event of a leak and spillage of sodium from an Intermediate Heat Transport System (IHTS) sodium loop, the pump in the loop will be shut down and the loop sodium will be drained into the dump tank in order to limit the mass of sodium that can spill and burn. The heat exchanger sodium channels must be large enough and oriented with a vertical component to enable efficient draining of sodium from the sodium channels. The heat exchanger sodium channels must also be large enough that sodium lenses that bridge individual channels and may remain inside of the heat exchanger after draining do not form. Air will enter the drained loop through the leak location and oxygen will oxidize any lens to form sodium oxide (Na_2O). Sodium oxide has a high melting temperature of about 1350 °C. It is not practical to melt out by heating an oxide plug that has formed due to the high oxide melting temperature. It might be possible to dissolve out a complete plug by washing it with relatively pure liquid sodium but such a process with a plug that completely blocks a channel must rely only on diffusive oxygen transport into the sodium mass adjacent to it. Because dissolution is limited by the diffusivity of oxygen in sodium, this process is very slow. Unplugging a completely plugged channel could take weeks or months. Thus, it isn't practical. In addition, the heat exchanger sodium channels must also be large enough to avoid plugging shut the heat exchanger due to the precipitation of sodium oxide at the cold end of the heat exchanger, in the event of a break in the cover gas system allowing air to enter the Argon cover gas of an IHTS loop with failure or shutdown of the intermediate sodium cold trap circuit.

The Argonne Sodium Draining and Refilling Tests are being conducted to demonstrate the efficient draining of sodium from vertical stainless steel channels having dimensions similar to the sodium channels in compact diffusion-bonded sodium-to-CO_2 heat exchanger designs. The tests are also revealing the fundamental phenomena involved when sodium drains from small vertically oriented stainless steel channels.

Sodium draining testing recently commenced with the first three sodium draining tests that involved draining sodium from a 0.46 m high 4.6 mm inner diameter stainless steel tube. Care was taken to ensure that the sodium wetted the stainless steel wall before each draining test. The stainless steel test section was filled with sodium, heated to 500 °C, and held at this temperature for 48 hours to assure wetting. Wetting was also verified by a significant decrease to a minimum in the voltage drop/electrical resistance across the test section outer diameter as measured by pairs of opposing electrodes welded to the test section outer surface.

Prior to the start of sodium testing, many shakedown tests were carried out using water. Some water tests used glass or plastic tubes facilitating visualization of the phenomena inside of the tubes. Three water draining tests utilized the same 4.6 mm inner diameter stainless steel tube. It

is thus possible to directly compare the results for sodium with water. Four other water tests used larger 7.7 and 10.2 mm inner diameter stainless steel tubes.

All of the water and sodium tests with stainless steel tubes have been analyzed and have revealed significant insights into the fundamental phenomena involved in draining of water and sodium.

The design and operation of the facility is described in Reference [1] together with a list of water draining tests that had been performed up until September 2017. This report discusses new water and sodium tests that have been performed with stainless steel tubes, the results of those tests, and analysis of the data. Recommendations and ideas for future testing are presented. A Summary of what has been learned from the test results and analysis is also provided.

2 Analysis of Water Draining Tests

An analysis has been carried out for the water draining tests performed using the three stainless steel test sections. Water tests were also carried out previously using glass and plastic tubes. The data from the glass and plastic tube tests has not been analyzed due to limitation of resources. In addition to the data measured during the tests, the water tests with glass and plastic tubes were important in providing experience in how to operate the facility and improve operations. A focus is made on those tests with the stainless steel test sections because it is possible to directly compare the data from those experiments to the data obtained with sodium draining from the same stainless steel test sections.

The authors of Reference [2] performed experiments similar to the Argonne draining tests in that fluids were drained from vertical tubes and collected atop a balance providing the mass collected versus time. Unlike the present experiments, the authors of Reference [2] were interested in highly viscous fluids such as honey for which the total draining time could be 200 seconds. They observed that the overall draining could be separated into four stages:

- Stage I: Plug flow. The air slug moves downwards and the tube empties of liquid at a constant rate. Videos indicated that the nose of the air slug travelled at a constant velocity, leaving an annular film of liquid behind. This stage ends when the air slug reaches the bottom of the tube at time, t_I;

- Stage II: Second linear stage. In several cases, Stage I was followed by a shorter period in which the drainage rate was constant. This stage ended at time, t_{II};

- Stages III and IV: Decreasing rate stages. After t_{II}, or t_I in cases where a second linear stage was not evident, the rate of drainage decreased with time. At some point the liquid ceased to drain as a steady filament and changed to a dripping regime, labelled IV. Small steps in the collected mass versus time are the result of droplet formation.

In the experiments of Reference [2], the slug draining in Stage I typically occurred in a laminar flow regime because of the high fluid viscosity.

Videos of glass and plastic tubes at Argonne during draining showed the rapid draining of a liquid water slug leaving behind a liquid water film upon the tube inner wall. Waves were observed to form upon the film and one could follow the downward descent of the waves and slow draining of remaining water over a timescale much longer than that of the slug draining.

It is not possible to observe the draining flow regimes inside of the stainless steel test sections. The only data available for draining of water are the load cell data and the high speed high definition videos of liquid draining into the collection cup atop the load cell. Examples of video frames from a 0.25 inch tube with an inner diameter of 4.572 mm (0.18 in) and tube height of 0.46355 m (18.25 in) are shown in Figure 1 and Figure 2. Because the draining water passes through the 10.16 mm (0.40 in) inner diameter 0.25 in tube segment and open ball valve below the test section, it is not possible to relate the flow regime of the draining liquid observed in the video to that of the liquid exiting the bottom of the test section. One observes a rapid draining phase in which the liquid water fills the inner diameter of the underlying tube segment. At some point, the liquid column starts to neck down. The point at which this begins to happen is subjective such that the time at which it happens may be uncertain. It is tempting to interpret this as roughly the end of the liquid slug draining phase. Subsequently, one observes rivulets and drops falling from the tube segment into the collection cup. While the recorded load cell data and videos from some tests were synchronized, some of them were not. For those tests, one cannot precisely match up a particular video frame with a particular time in the load cell output dataset. One can roughly match the frame at which draining liquid is first observed to the time when the load cell data starts exhibiting a rise.

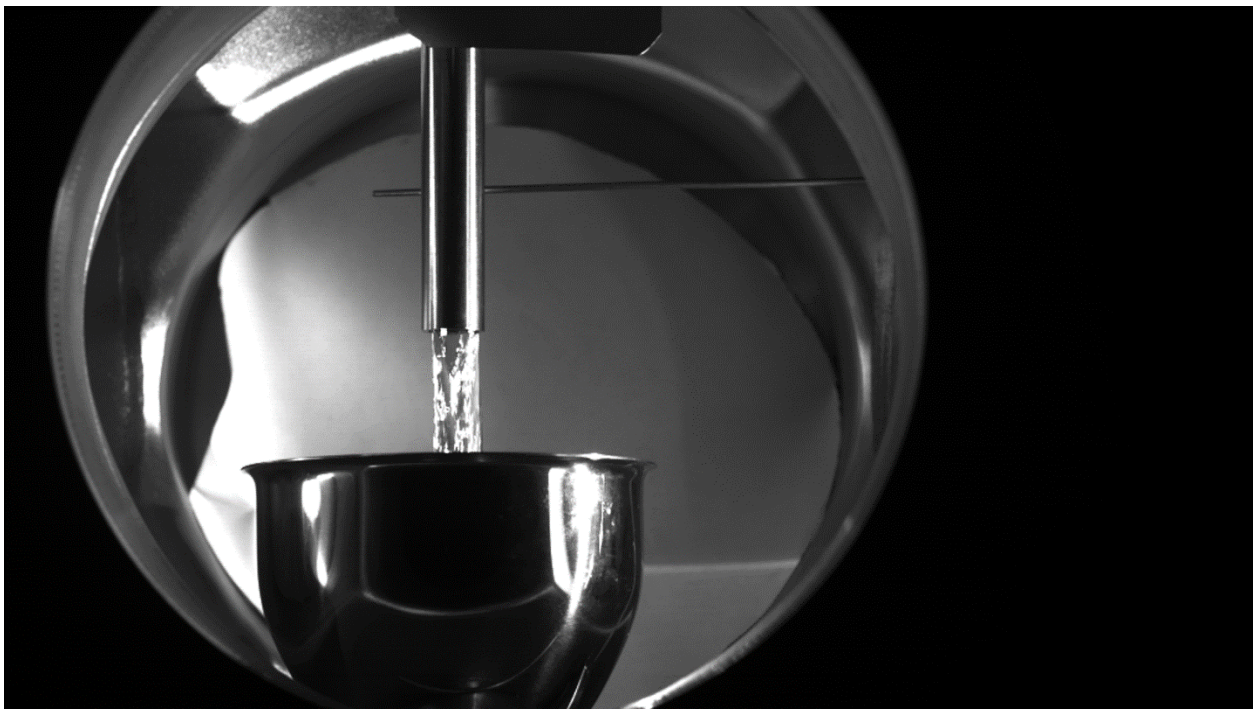

Figure 1. High Speed High Definition Video Frame for Water Draining from 0.25 inch Stainless Steel Tube with 4.572 mm (0.18 in) Inner Diameter.

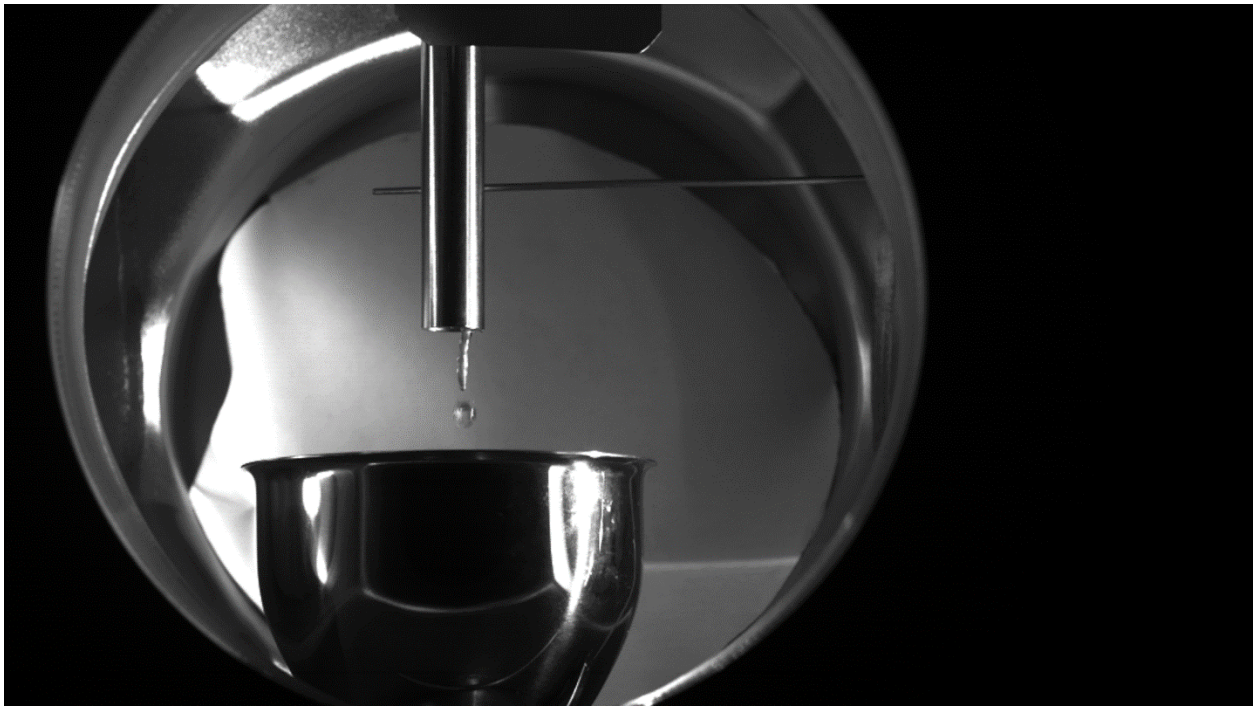

Figure 2. High Speed High Definition Video Frame for Water Draining from 0.25 inch Stainless Steel Tube with 4.572 mm (0.18 in) Inner Diameter.

For this analysis, the load cell data is principally relied upon. Unfortunately, the load cell data does not provide a clear measurement of the mass collected versus time. First, the load cell responds to both the weight of collected liquid and the impact force of the draining liquid transmitted to the steel wool in the collection cup. Second, the load cell, collection cup, steel wool, and collected liquid mass are a dynamical system with an oscillatory behavior when excited by impacting liquid. The resulting load cell output exhibits damped oscillations. The amplitude of the oscillations is greater when the liquid draining rate is greater.

Raw data from the load cell exhibits a lot of oscillations. Prominent is an oscillation around 70 Hz suggestive of the effects of the 60 Hz line current. The load cell comes with a capability to electronically filter out frequencies above a specified frequency cutoff from the output. The resulting output that is recorded is filtered; the unfiltered data is lost. A filter with a cutoff of 10 Hz was used during the water tests. Thus, all frequencies above 10 Hz were removed. This filtering definitely improves the data and aids in interpretation of results.

The filtered load cell output for water draining from a 0.25 inch tube with an inner diameter of 4.572 mm (0.18 in) and tube height of 0.46355 m (18.25 in) are shown in Figure 3 through Figure 5. The start time on the figures is arbitrary. The mass that drains is not just the mass contained in the tube. It also includes the liquid mass initially filling the 0.12065 m (4.75 in) tube segment between the bottom of the tube and the closure of the ball valve. It is observed that all of the liquid mass drains in just a few seconds (Figure 3). By 6 seconds, the drained mass has essentially reached the total value. The load cell oscillations have died out. By averaging the

load cell output at the end of the recorded data over time, one can average out noise effects and obtain an accurate value for the total mass drained.

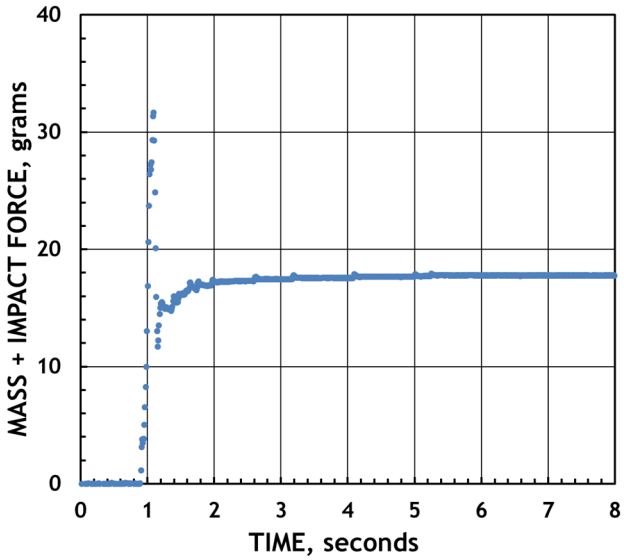

Figure 3. Load Cell Output versus Time for Test WSST025 1 for Water Draining from 0.25 inch Stainless Steel Tube with 4.572 mm (0.18 in) Inner Diameter.

Figure 4 shows the early time behavior during the rapid draining phase. The load cell output rises to a peak and falls to a minimum. As shown in Figure 3, the output exceeds the total mass. This is the dynamic behavior of the load cell system whereby the output overshoots the impact force plus mass. The load cell system then "snaps back" and undershoots the impact force plus mass at the minimum.

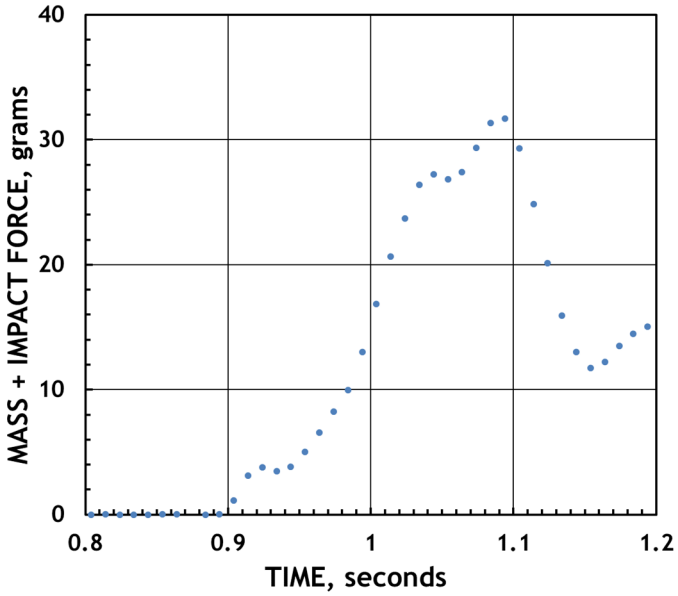

Figure 4. Load Cell Output versus Time for Test WSST025 1 for Water Draining from 0.25 inch Stainless Steel Tube with 4.572 mm (0.18 in) Inner Diameter.

Of interest is the liquid mass drained during the rapid draining phase. It is assumed here that the time at the end of the rapid draining phase can be estimated as the time at which the undershoot minimum occurs at 1.15 s on Figure 4. Figure 5 focuses on the subsequent load cell output. It is observed that there is a second phase during which the liquid drains at an approximately linear rate as discussed in Reference [2]. After the linear rate phase, the drained mass increases at a more gradual deceasing rate as also discussed in Reference [2].

To estimate the mass drained during the rapid draining phase, a curve is "eyeballed" through the data during the linear phase in Figure 5 and extrapolated back to the time of the undershoot minimum. Eyeballing is also used to extrapolate the linear rate data forward to estimate a mass when the linear draining rate phase ends. Admittedly, this is subjective but it is probably as good as any other approach to dealing with the uncertainty inherent in the load cell output.

Several spikes are observed from just before 2 seconds to 6 seconds. These are impacts from individual rivulets or drops.

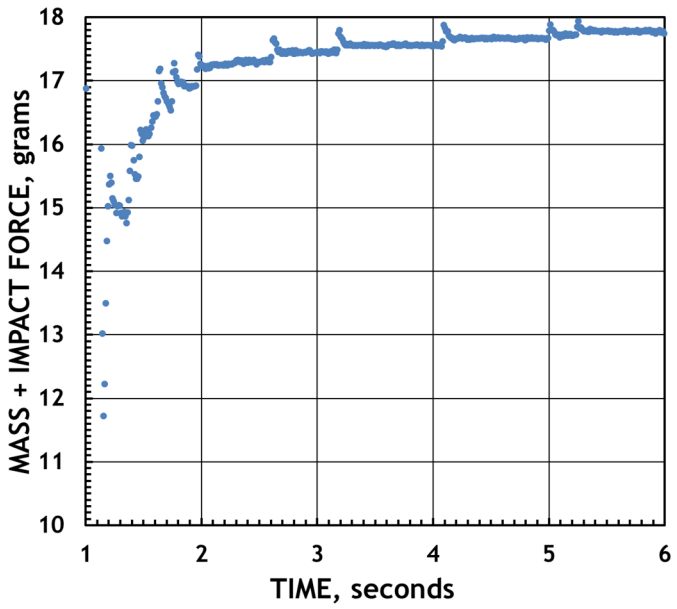

Figure 5. Load Cell Output versus Time for Test WSST025 1 for Water Draining from 0.25 inch Stainless Steel Tube with 4.572 mm (0.18 in) Inner Diameter.

For this example, the time averaged total mass is 17.76 g, the estimated mass drained during the rapid draining phase is 14.3 g, and the mass drained after the linear rate phase is 17.2 g. From these masses, it is necessary to subtract off the liquid mass drained from the space between the bottom of the tube and the ball valve. Six water draining tests were run without any tube above the underlying 10.16 mm (0.40 in) inner diameter tube segment. For each run, the time averaged total mass drained was determined and the six values were averaged. The resulting water mass is 10.01 g. Thus, from just the 4.572 mm inner diameter tube, the estimate of the total mass drained is 7.751 g, the mass rapidly drained is 4.29 g, and the mass drained up to the end of the linear rate phase is 7.19 g. The mass fraction rapidly drained from the tube is 0.553. The mass fraction drained from the tube through the rapid and linear rate draining phases is 0.927.

From Figure 4, the rapid draining phase is estimated to last 1.15-0.895 s = 0.255 s. From the video, the rapid draining phase is estimated roughly as 0.21 s. The end of the linear draining rate phase from Figure 5 is estimated to occur at 1.85 s. Thus, the linear draining rate phase is estimated to be 1.85 – 1.15 s = 0.70 s long. The sum of the rapid and linear rate draining times is 0.955 s. 92.7 % of the liquid drains from the tube in this time. The remaining 7.3 % drains more slowly over the next 4 seconds.

Overall, all of the water has drained from the tube by 6 seconds. This is an important and good result implying that a vertically-oriented heat exchanger with 4.6 mm diameter vertical liquid channels 0.46 m high can be drained in only 6 seconds. Most of the liquid drains from the channels in the first second. For such a heat exchanger, a 4.6 mm channel size is large enough to permit efficient draining of liquid.

Seven water draining tests were conducted with the stainless steel tubes. For each test, an analysis similar to that described above was performed. The results are shown in Table 1. For each tube size, differences are observed between the different tests. The differences in large part include the effects of uncertainties in the load cell data and the approach to estimating masses by eyeballing plots of the load cell data. Main results of interest include the fraction of liquid water remaining inside of the tube following the end of the linear rate draining phase. The data indicates that the remaining mass fraction increases as the tube inner diameter decreases especially for the 4.572 mm tube. The remaining mass fractions are small ranging from 0.073 to 0.125 for the 4.572 mm tube. Significantly greater fractions of water are left in the tubes at the end of the rapid liquid slug draining phase. Values range from 0.438 to 0.560 for the 4.572 mm tube. The rapid draining phase times estimated from the videos differ from those estimated from plots of the load cell data. The reason for the large difference in rapid draining times for Test WSST0375 1 is not known. The sum of the rapid and linear rate phase draining times increase as the tube diameter increases but are still of the order of one second for the three tubes. Total draining times for all of the liquid increase from 6 s for the 4.572 mm tubes to 9 s for the 10.16 mm tubes.

Table 1. Results for Water Draining Tests with Stainless Steel Tubes

Test	WSST0251	WSST0252	WSST0253	WSST0375 1	WSST0375 2	WSST0501	WSST0502
Tube ID, mm (in)	4.572 (0.18)	4.572 (0.18)	4.572 (0.18)	7.747 (0.305)	7.747 (0.305)	10.16 (0.40)	10.16 (0.40)
Tube Height, m (in)	0.46355 (18.25)	0.46355 (18.25)	0.46355 (18.25)	0.46355 (18.25)	0.46355 (18.25)	0.46355 (18.25)	0.46355 (18.25)
Rapid Draining Time from Load Cell Plots, s	0.255	0.230	0.265	0.295	0.295	0.252	0.262
Rapid Draining Time from Video, s	0.21	0.15	0.16	0.61	0.22	0.27	0.31
Linear Draining	0.70	0.78	0.62	0.99	0.66	1.11	0.89

Rate Phase Draining Time from Load Cell Plot, s							
Rapid Plus Linear Rate Phase Draining Time from Load Cell Plots, s	0.955	1.01	0.885	1.285	0.955	1.37	1.15
Total Draining Time, s	6	6	6	8	8	9	9
Total Mass Drained, g	17.76	18.00	17.70	31.74	31.95	48.18	48.05
Mass Drained During Rapid Phase, g	14.3	14.5	13.4	27.3	27.3	43.0	42.4
Mass Drained During Rapid Phase Plus Linear Rate Phase, g	17.2	17.0	17.0	30.4	30.7	46.0	46.0
Total Mass Drained from Tube, g	7.751	7.985	7.689	21.7	21.9	38.2	38.0
Mass Drained from Tube During Rapid Phase, g	4.29	4.49	3.39	17.3	17.3	33.0	32.5
Mass Drained from Tube During Rapid Phase Plus Linear Rate Phase, g	7.19	6.99	6.99	20.4	20.7	36.0	36.0
Mass Fraction Drained from Tube During Rapid Phase	0.553	0.562	0.440	0.796	0.788	0.864	0.854
Mass Fraction Drained from Tube During Rapid Phase Plus Linear Rate Phase	0.927	0.875	0.909	0.938	0.943	0.943	0.946
Mass Fraction Remaining in Tube After Rapid Phase	0.447	0.438	0.560	0.204	0.212	0.136	0.146

Mass Fraction Remaining in Tube After Rapid Phase Plus Linear Rate Phase	0.073	0.125	0.091	0.062	0.057	0.057	0.054
For 10.16 mm Inner Diameter Test Section, Mass Fraction Drained During Rapid Phase from Both Test Section and Underlying Tube Segment						0.892	0.885
For 10.16 mm Inner Diameter Test Section, Mass Fraction Drained During Rapid Plus Linear Rate Phases from Both Test Section and Underlying Tube Segment						0.955	0.957
For 10.16 mm Inner Diameter Test Section, Mass Fraction Remaining After Rapid Phase in Both Test Section and Underlying Tube Segment						0.108	0.115
For 10.16 mm Inner Diameter Test Section,						0.045	0.043

Mass Fraction Remaining After Rapid Plus Linear Rate Phases in Both Test Section and Underlying Tube Segment							
Mean Velocity Estimated Using Rapid Draining Time from Load Cell Data Plots, m/s	2.29	2.54	2.20	1.98	1.98	2.32	2.23
Reynolds Number for Mean Velocity	10,400	11,600	10,000	15,300	15,000	23,500	22,600
Capillary Number	0.0315	0.0350	0.0304	0.0273	0.0273	0.0319	0.0307
Water Mass Fraction Remaining in Tube Predicted Using Horizontal Tube Correlation	0.178	0.187	0.174	0.165	0.165	0.179	0.175

Figure 6 through Figure 8 and Figure 9 through Figure 11 show the load cell data plots for draining from one each of the 7.747 mm (0.305 in) and 10.16 mm (0.40 in) inner diameter tubes, respectively. Load cell system dynamic oscillations are observed to be more pronounced during the linear rate draining phase than for the 4.572 mm (0.18 in) inner diameter tube.

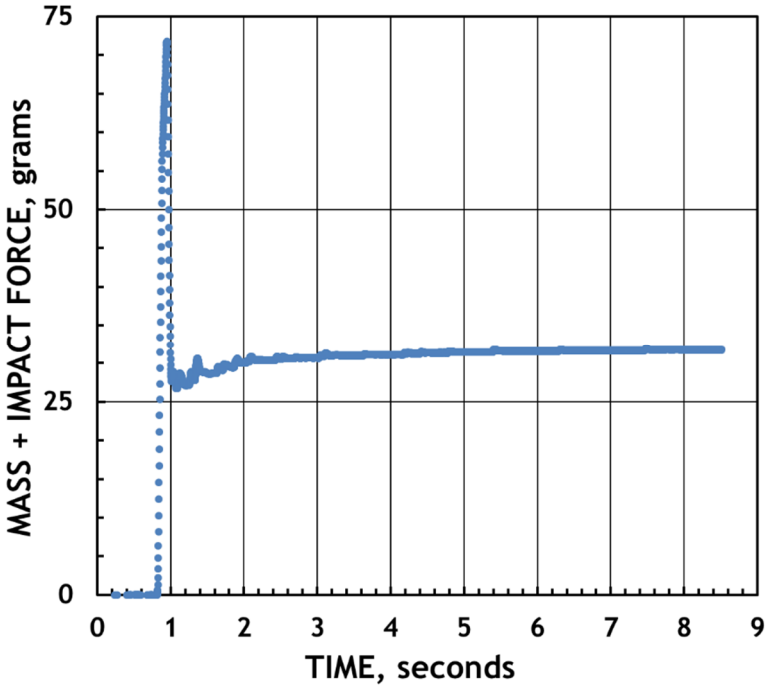

Figure 6. Load Cell Output versus Time for Test WSST0375 1 for Water Draining from 0.375 inch Stainless Steel Tube with 7.747 mm (0.305 in) Inner Diameter.

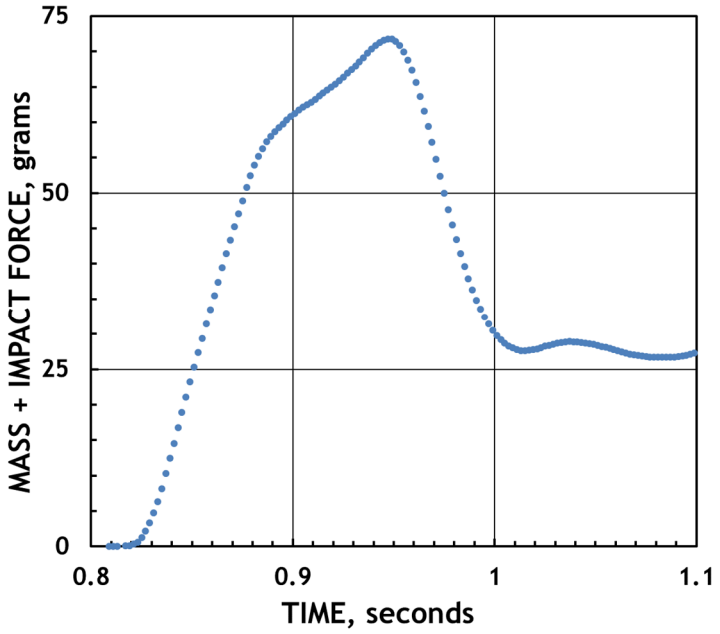

Figure 7. Load Cell Output versus Time for Test WSST0375 1 for Water Draining from 0.375 inch Stainless Steel Tube with 7.747 mm (0.305 in) Inner Diameter.

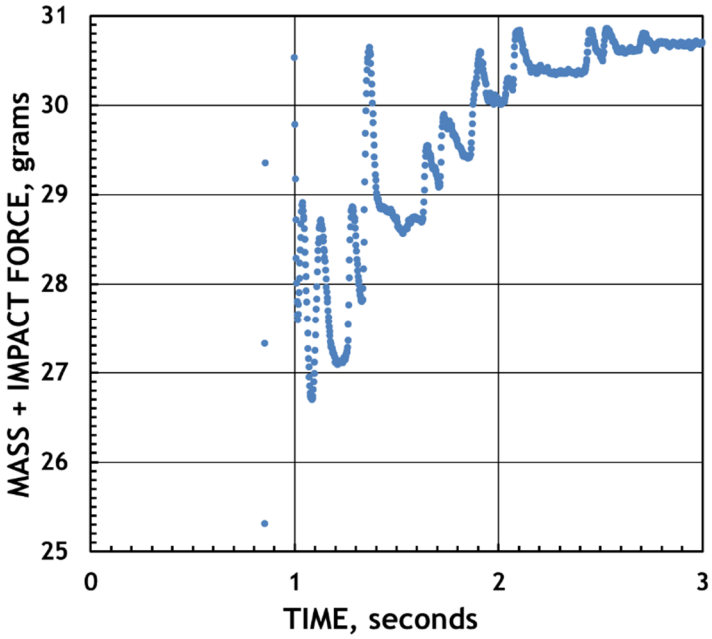

Figure 8. Load Cell Output versus Time for Test WSST0375 1 for Water Draining from 0.375 inch Stainless Steel Tube with 7.747 mm (0.305 in) Inner Diameter.

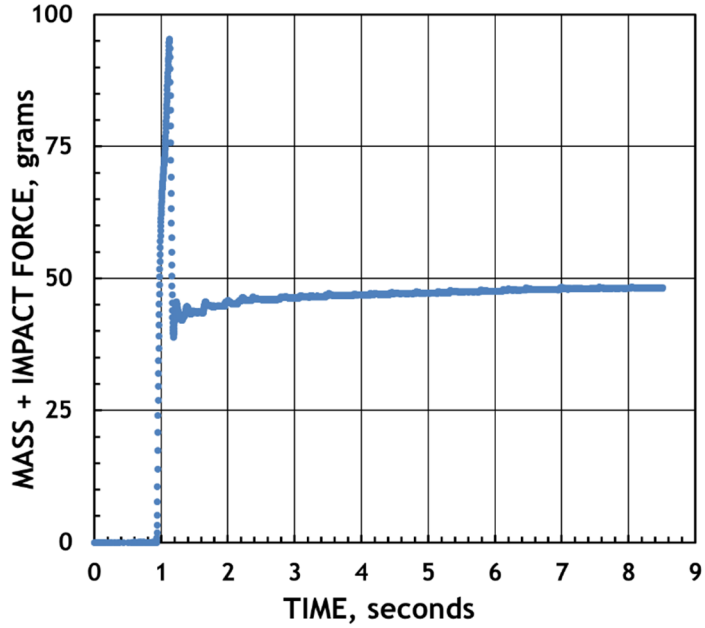

Figure 9. Load Cell Output versus Time for Test WSST050 1 for Water Draining from 0.50 inch Stainless Steel Tube with 10.16 mm (0.40 in) Inner Diameter.

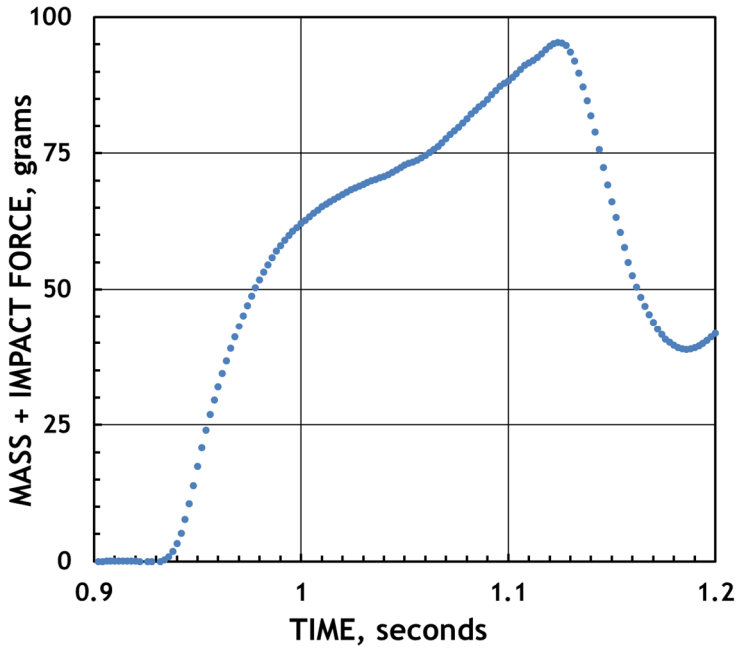

Figure 10. Load Cell Output versus Time for Test WSST050 1 for Water Draining from 0.50 inch Stainless Steel Tube with 10.16 mm (0.40 in) Inner Diameter.

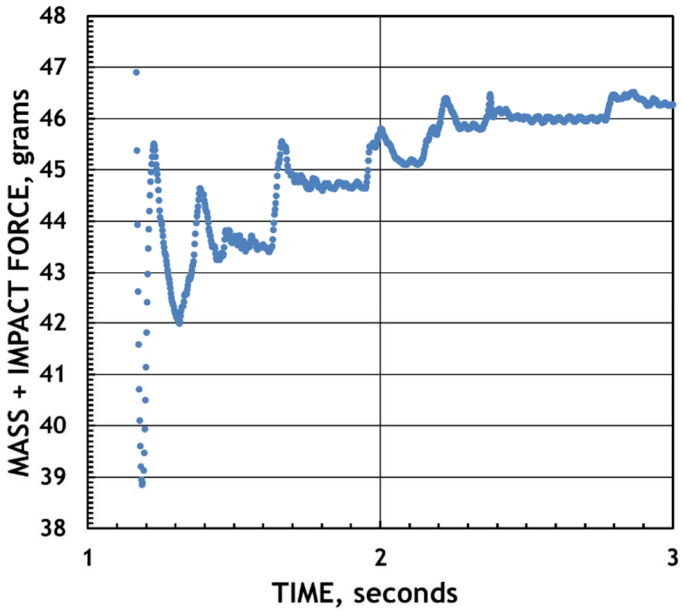

Figure 11. Load Cell Output versus Time for Test WSST050 1 for Water Draining from 0.50 inch Stainless Steel Tube with 10.16 mm (0.40 in) Inner Diameter.

For the tests using the 0.5 in test section with an inner diameter of 10.16 mm (0.4 in) and only for the tests using this test section, the tube inner diameter is identical to that of the underlying tube segment above the ball valve. Figure 12 shows the VCR connections welded to the 0.375 and 0.50 inch test sections. For the 10.16 mm inner diameter test section, the circular channel is essentially unchanged going through the connection. Thus, one can also view these tests as

draining of water from a tube having a greater height of 0.5842 m (18.25+4.75 in = 23 in). For these tests, the masses collected from both the test section and the underlying tube segment can also be used to estimate mass fractions. The results are included in Table 1. The mass fractions calculated without and with the underlying tube segment are different but the differences are not large. The present values for draining from a greater tube height are preferred.

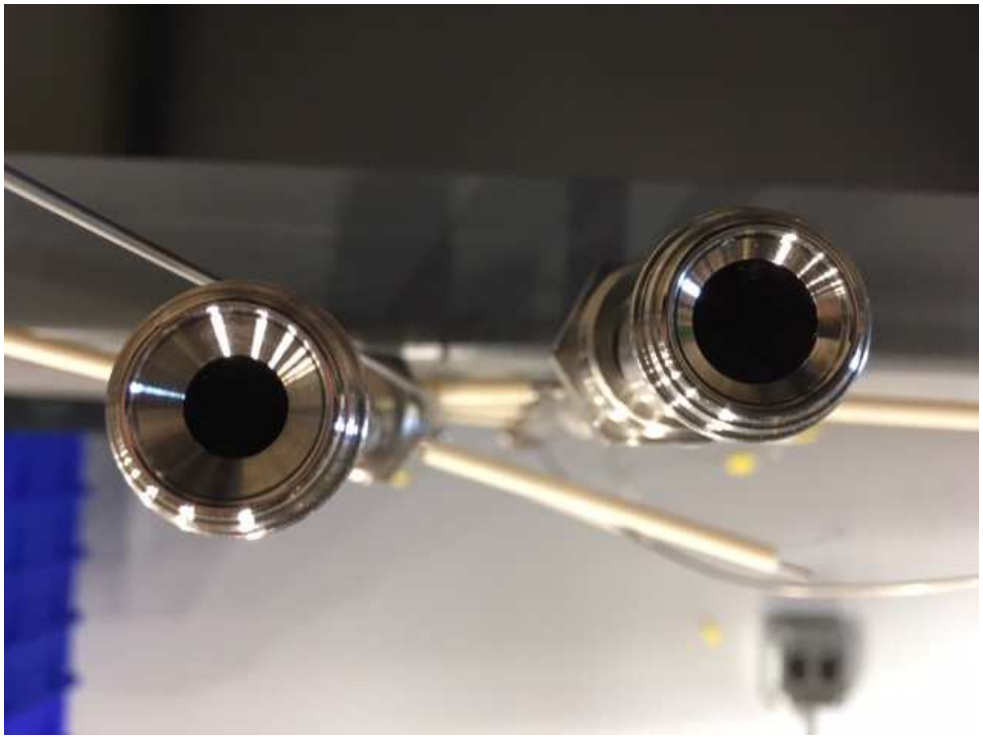

Figure 12. End View of VCR Fittings on 0.375 and 0.50 inch Test Sections.

When a gas is blown down a horizontal tube, a round-ended column is formed that travels down the tube forcing some liquid out at the far end and leaving a fraction, x, in the form of a layer covering the wall. Fairbrother and Stubbs [3] conducted experiments with fluids generally having low viscosities. They found that the fraction of liquid mass, x, remaining inside of the tube could be correlated as

$$x = \left(\frac{\mu U}{\sigma}\right)^{\frac{1}{2}}$$

where μ = viscosity, U = velocity of bubble penetrating into the liquid, and σ = surface tension. The non-dimensional group is known as the Capillary number. Sir Geoffrey Taylor [4] extended the correlation to fluids having high viscosities presenting a curve that is a function of the Capillary number non-dimensional group. The above correlation holds for Capillary numbers below about 0.1. He noted that the coincidence that the leading coefficient is equal to unity was not explained.

The correlation was applied to the water draining tests for the rapid liquid slug draining phase when the liquid initially fills the tube. The liquid slug velocity was not measured for any of the tests. A mean velocity was estimated by dividing the total fall height equal to the height of the

tube plus the underlying tube segment above the ball valve by the rapid draining time determined from the load cell data plots. The total fall height is 0.5842 m (18.25+4.75 in = 23 in). Water at 20 °C was assumed for which ρ= 998.2 kg/m^3, μ= 1.002×10^{-3} Pa·s, and σ = 0.0727 N/m.

The results are included at the bottom of Table 1. The estimated mean velocities correspond to turbulent flow as the liquid slug drains. The correlation for the mass remaining inside of a horizontal tube is independent of the tube diameter. The predicted values for the seven tests range from 0.165 to 0.187 with an average for the seven tests of 0.175. The predictions differ significantly from the observed mass fractions remaining after the rapid draining phase and after the rapid plus linear rate draining phases. For the 4.572 mm inner diameter tubes, the correlation predicts values significantly less than the observed mass fraction remaining after the rapid draining phase and significantly greater than after the rapid plus linear rate draining phases. The differences between the correlation predictions and the Argonne water draining data indicate a fundamental difference in the phenomena of emptying liquid from tubes in vertical orientation versus horizontal orientation.

The correlation provides a context in which to compare sodium with water. Assume sodium at 332.2 °C for which ρ= 873.2 kg/m^3, μ= 3.171×10^{-4} Pa·s, and σ = 0.1761 N/m. The sodium viscosity is significantly lower than that of water and the sodium surface tension is significantly greater. Assume a mean sodium velocity of 2.26 m/s. The capillary number for sodium is 0.00408 versus 0.0312 for water assuming the same velocity. The predicted remaining mass fraction of sodium in a horizontal tube is 0.0639. This is significantly lower than that predicted for water which is 0.177 assuming the same velocity. On this basis, one might expect significantly less sodium to remain inside of a vertical tube after the rapid and linear rate draining phases compared to water.

One of the purposes of the Argonne Draining and Refilling Tests is to determine the minimum sodium channel size above which sodium can be readily drained from a sodium channel. Jensen in Reference [5] proposed a criterion for the minimum vertical tube size below which liquid lenses could form across the channel. This is exactly the type of criterion that is sought to determine if sodium can remain inside of a channel forming bridges across the channel. Jensen formulated his criterion in terms of a Bond number,

$$\mathrm{Bo} = \frac{\rho g a^2}{\sigma \varepsilon},$$

where ρ = density, g = gravitational acceleration, a = tube inner radius, and εa = thickness of the liquid film on the wall immediately ahead of the collar or lens. Jensen proposed the following criteria:

- For 0<Bo<0.5960, all draining collars grow in volume and, in sufficiently long tubes, ultimately “snap off” to form stable lenses;
- For 0.5960<Bo<1.769, small collars may shrink but in long tubes sufficiently large collars will snap off;

- For 1.769<Bo<11.235, both stable collars and lenses may arise, although most collars will shrink; and

- If Bo>11.235, all collars and lenses shrink in volume as they drain, so that any lens ultimately ruptures, unless stabilizing intermolecular forces allow the formation of a lamella supported by a macroscopic Plateau border.

The criteria imply that stable lenses form for Bond numbers below 1.769 from snapping off of collars. Above this critical Bond number, most collars will shrink and not form stable lenses.

The radius fraction, ε, is calculated from the mass fraction, x, as

$$\varepsilon = 1 - (1 - x)^{\frac{1}{2}} \ .$$

The mass fraction predicted by the correlation for a horizontal tube is assumed here. The rationale is that it depends upon fluid properties and can be used to compare sodium and water. The critical diameter varies with the square root of the radius fraction which makes it somewhat less sensitive to the actual value. Assuming a water mass fraction of 0.177, the radius fraction is 0.0926. The critical radius is calculated as 1.10 mm such that the critical diameter is 2.21 mm. Thus, it is predicted that water will not efficiently drain from a vertical tube with a diameter below 2.21 mm.

The calculation was repeated for sodium. Assuming a sodium mass fraction of 0.0639, the radius fraction is 0.0325. The critical radius and diameter are 1.09 and 2.17 mm, respectively. The critical diameter for sodium is predicted to be slightly less than that for water.

Ideally, one would like to perform draining tests with water and sodium with a 2 mm inner diameter tube. A stainless steel tube this size was not procured because a supplier that also provides a material certification required for sodium work at Argonne could not be located. However, performing a draining test with such a small tube presents practical difficulties. Assuming that the tube height is the same as for the existing three stainless steel tubes, the water mass inside of a filled tube is less than 1.5 g. Using the current experiment setup with the tube segment between the bottom of the tube and ball valve will not provide accurate data. The much larger mass of liquid in the segment below the tube and above the ball valve amounting to 10.01 g for water as well as the errors inherent in the load cell data will make it impractical to determine masses that might drain during rapid draining and linear rate draining phases because one would be taking small differences of relatively large numbers. To carry out meaningful draining tests with a 2 mm inner diameter tube, a new experiment approach is required that is tailored to the small draining mass involved.

Incidentally, in correlating the mass fraction data from the Argonne draining tests, one would seek a correlation involving both the Capillary number and a Bond number.

3 Analysis of Sodium Draining Tests

Sodium draining tests were carried out using the 4.572 mm inner diameter stainless steel tube. In general, the data shows that sodium drains much more efficiently than water. This was expected from the Capillary number correlation discussed above but the extent of the difference between sodium and water was surprising. The rapid slug draining time for the first sodium test is estimated as only 0.16 s for sodium versus 0.25 s for water. The shorter slug draining time implies a higher slug velocity that implies a higher impact pressure. Because this is the first sodium draining test, there was no sodium from previous tests inside of the catch cup. The greater impact pressure combined with the low mass atop of the load cell resulted in more vigorous overshoots in the load cell output as shown in Figure 13 through Figure 16.

The load cell data do not clearly show a separate linear rate draining phase following the rapid slug draining phase. Instead, there is a rapid slug draining phase followed by a slow rate draining phase. The load cell data indicate that a significant discrete mass of sodium subsequently drains into the catch cup during the slow rate draining phase in a single event at about 3.55 s. This behavior was not observed in any of the water tests that involved draining of several rivulets and drops. The high speed high definition video camera was not available for the sodium draining tests. An example of a normal speed video frame is shown in Figure 17. The draining metallic sodium surface is observed to be smooth reflecting images similar to stainless steel. The video does not reveal any information about the discrete draining event at 3.55 s. This may be due to an inability to stop the motion of rivulets and drops none of which could be discerned on the video. Because the flowpath involves flow through the ball valve and underlying tube segment, it is not possible to attribute this increase in the load cell output to an event strictly inside of the 4.572 mm inner diameter tube.

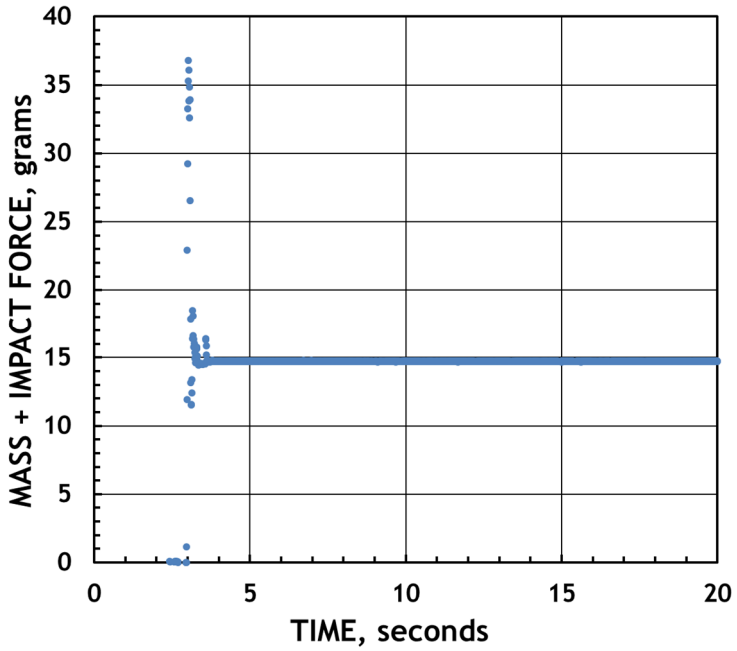

Figure 13. Load Cell Output versus Time for Test SSST025 1 for Sodium Draining from 0.25 inch Stainless Steel Tube with 4.572 mm (0.18 in) Inner Diameter.

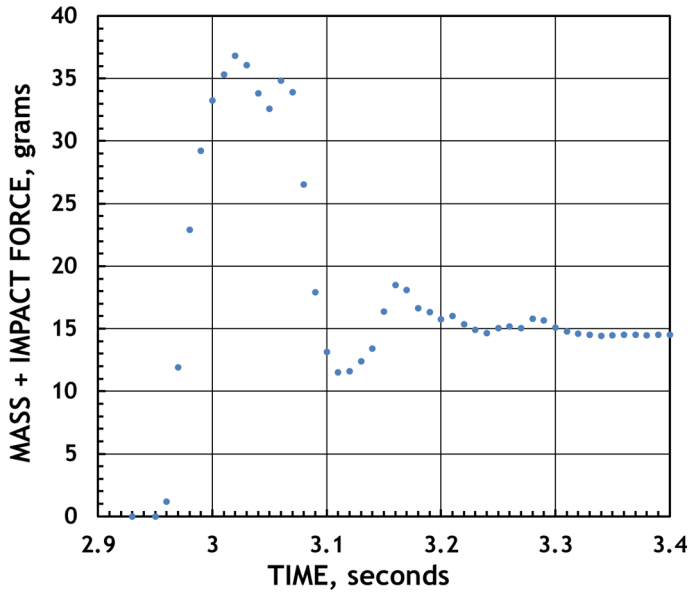

Figure 14. Load Cell Output versus Time for Test SSST025 1 for Sodium Draining from 0.25 inch Stainless Steel Tube with 4.572 mm (0.18 in) Inner Diameter.

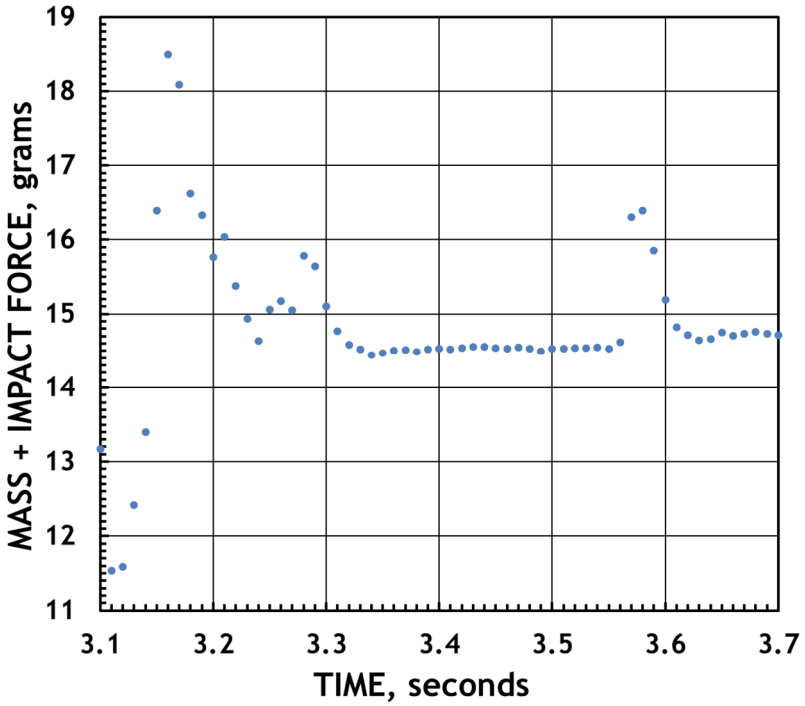

Figure 15. Load Cell Output versus Time for Test SSST025 1 for Sodium Draining from 0.25 inch Stainless Steel Tube with 4.572 mm (0.18 in) Inner Diameter.

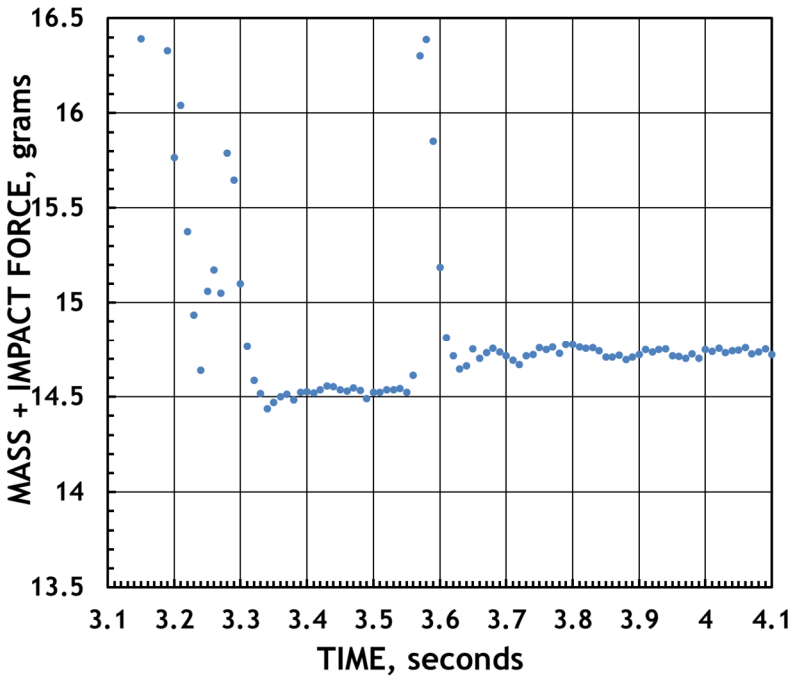

Figure 16. Load Cell Output versus Time for Test SSST025 1 for Sodium Draining from 0.25 inch Stainless Steel Tube with 4.572 mm (0.18 in) Inner Diameter.

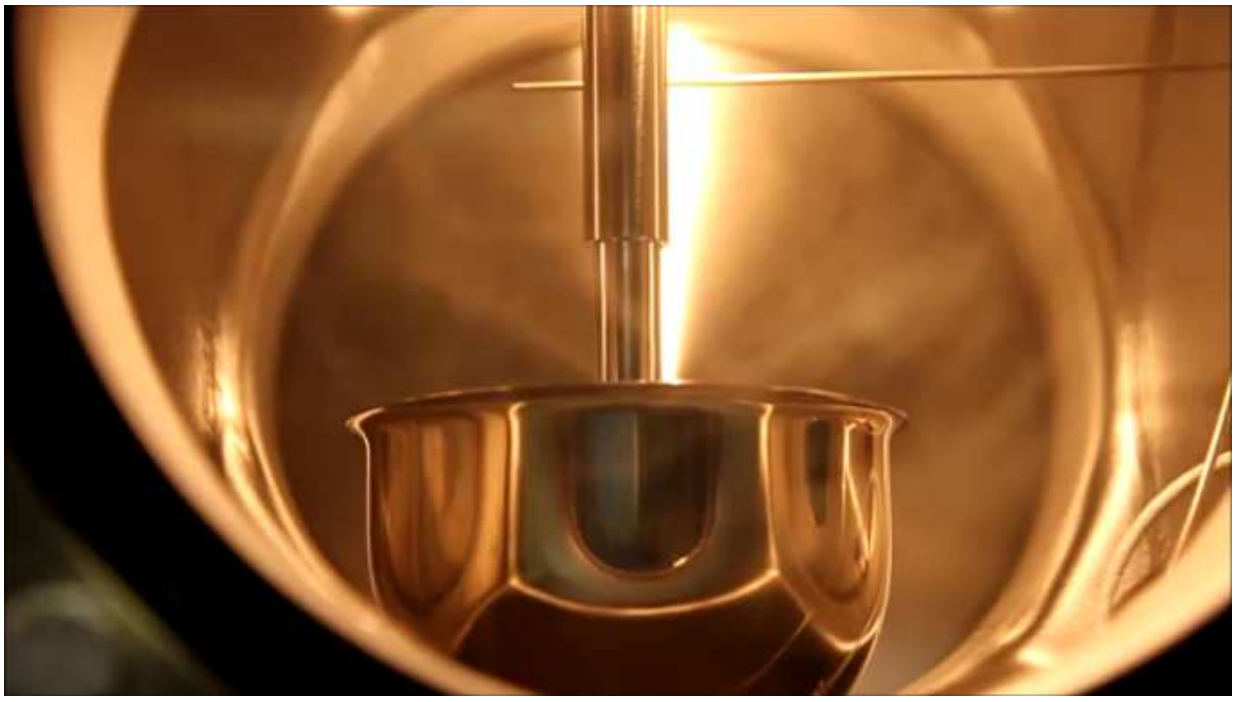

Figure 17. Video Frame for Sodium Draining from 0.25 inch Stainless Steel Tube with 4.572 mm (0.18 in) Inner Diameter in Test SSST025 1.

The vigorous overshooting of the load cell dynamic system led to the realization that the mass atop the load cell should be increased. This could be accomplished by hanging weights from the brim of the catch cup. Unfortunately, it was not possible to do this after the first sodium test because it would have been necessary to open up the six-way cross.

A second sodium test was performed with the objective of draining sodium at the identical conditions as in the first test. The objective was to explore if similar results were obtained such as the discrete draining event at about 3.55 s. The load cell output would not be identical due to the small mass of sodium inside of the catch cup from the first sodium test. Unfortunately, in pushing sodium up into the stainless steel tube, significantly more sodium was pushed up into the tube than needed to just fill the tube. This was not a significant shortcoming of the test as the phenomena involving a liquid film left behind the descending slug trailing edge should be similar. No discrete draining event later in time was observed for seventeen seconds. Figure 18 through Figure 21 show the load cell output. The total mass collected is 24.015 g versus 14.732 g in the first sodium test. The mass estimated to fill just the height of the tube is 6.8295 g assuming sodium at 225 °C having a density of 897.4 kg/m^3. The oscillations in the load cell output are particularly evident during the rapid slug draining phase where four local peaks and four local troughs are observed.

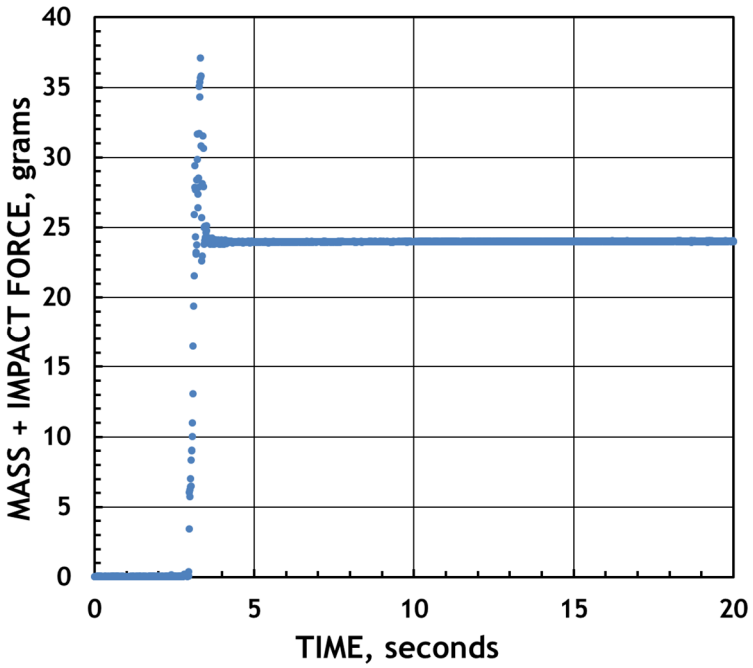

Figure 18. Load Cell Output versus Time for Test SSST025 2 for Sodium Draining from 0.25 inch Stainless Steel Tube with 4.572 mm (0.18 in) Inner Diameter.

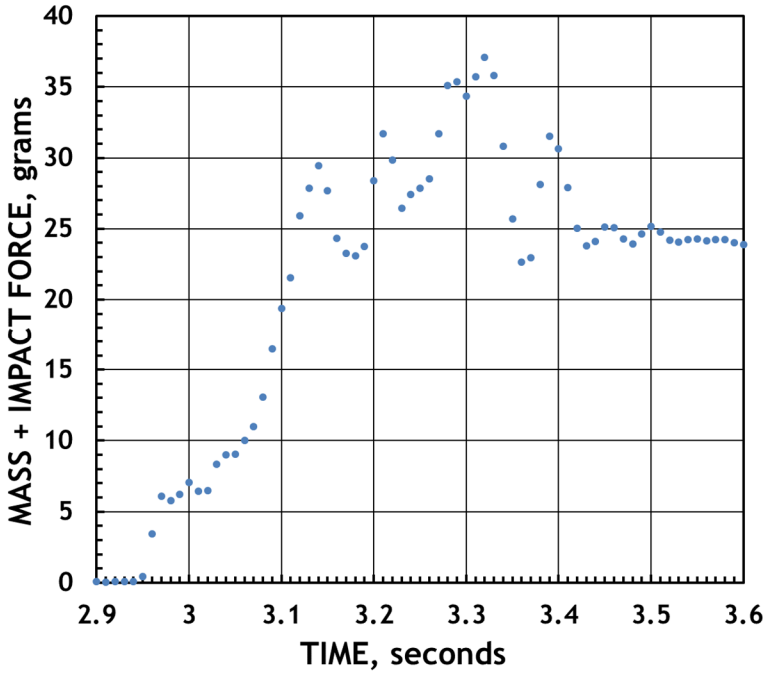

Figure 19. Load Cell Output versus Time for Test SSST025 2 for Sodium Draining from 0.25 inch Stainless Steel Tube with 4.572 mm (0.18 in) Inner Diameter.

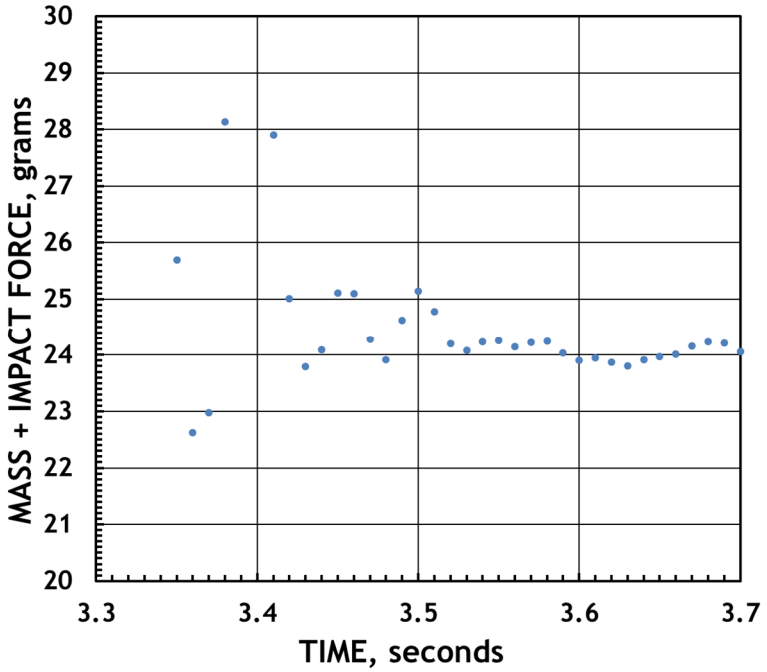

Figure 20. Load Cell Output versus Time for Test SSST025 2 for Sodium Draining from 0.25 inch Stainless Steel Tube with 4.572 mm (0.18 in) Inner Diameter.

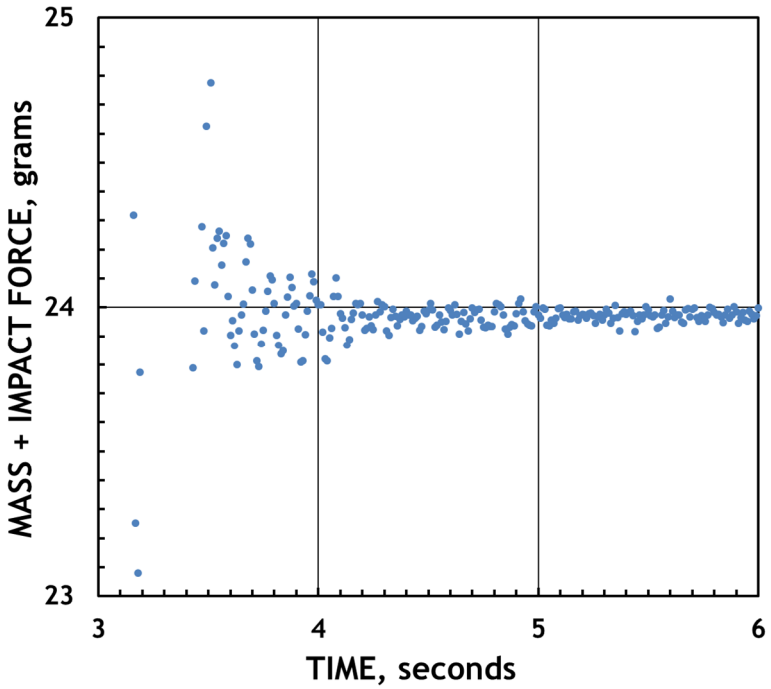

Figure 21. Load Cell Output versus Time for Test SSST025 2 for Sodium Draining from 0.25 inch Stainless Steel Tube with 4.572 mm (0.18 in) Inner Diameter.

A third sodium test was performed with the objective of only filling the tube to the top. However, it was also overfilled similarly to the second sodium test. The load cell data are shown in Figure 22 through Figure 26. Similar to the first sodium draining test, a single discrete draining event is observed later in time at 8.9 s. Although such a discrete event is not prominent in the data from the second sodium test, it is possible that it occurred in the second sodium test at 3.4 s at the end of the rapid slug draining phase or after twenty seconds when data recording had stopped.

Although it was confirmed that the load cell voltage output was filtered using a 10 Hz cutoff, the load cell data exhibits prominent oscillations above 10 Hz. In particular, oscillations at 28 Hz and 70 Hz can be seen. The reason why these oscillations were not eliminated is unknown. This oscillation behavior is similar to that observed in some water tests where the oscillations became similarly more pronounced as the catch cup filled with water.

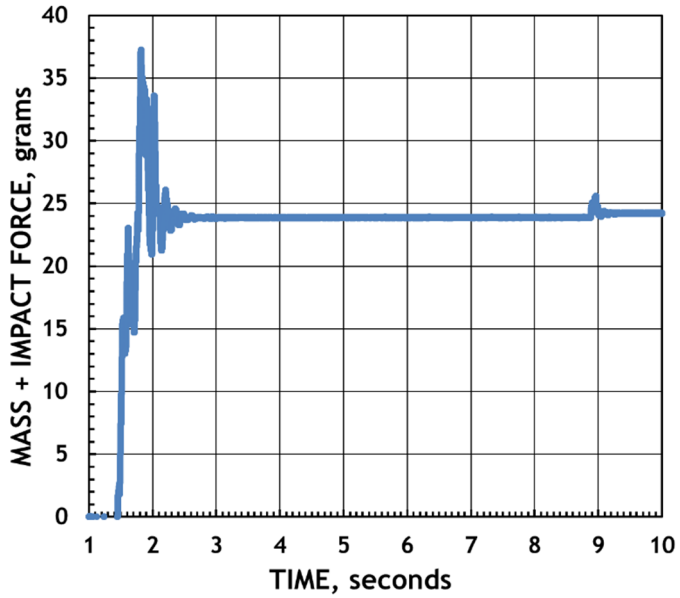

Figure 22. Load Cell Output versus Time for Test SSST025 3 for Sodium Draining from 0.25 inch Stainless Steel Tube with 4.572 mm (0.18 in) Inner Diameter.

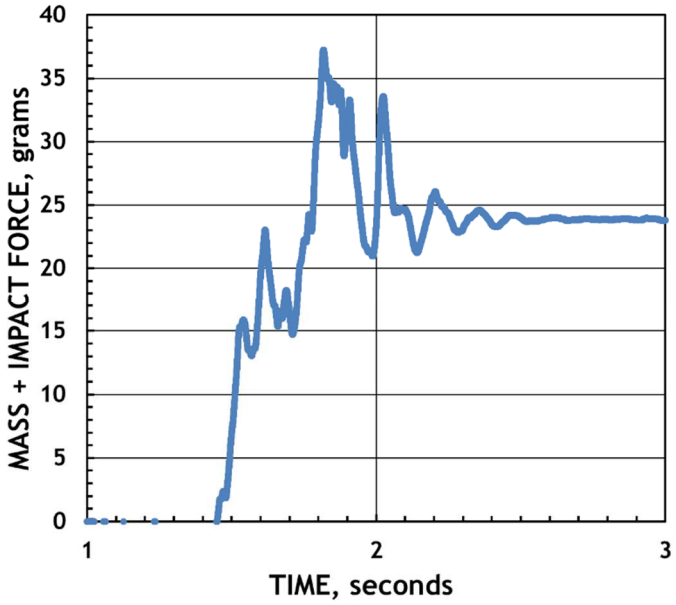

Figure 23. Load Cell Output versus Time for Test SSST025 3 for Sodium Draining from 0.25 inch Stainless Steel Tube with 4.572 mm (0.18 in) Inner Diameter.

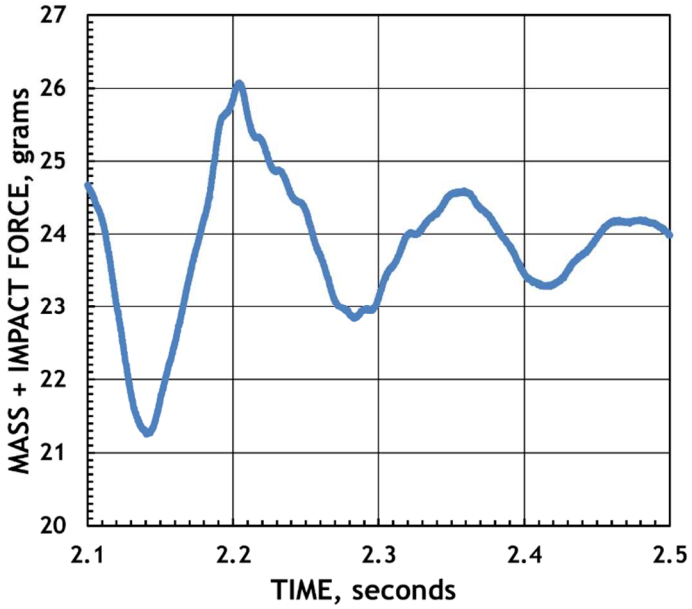

Figure 24. Load Cell Output versus Time for Test SSST025 3 for Sodium Draining from 0.25 inch Stainless Steel Tube with 4.572 mm (0.18 in) Inner Diameter.

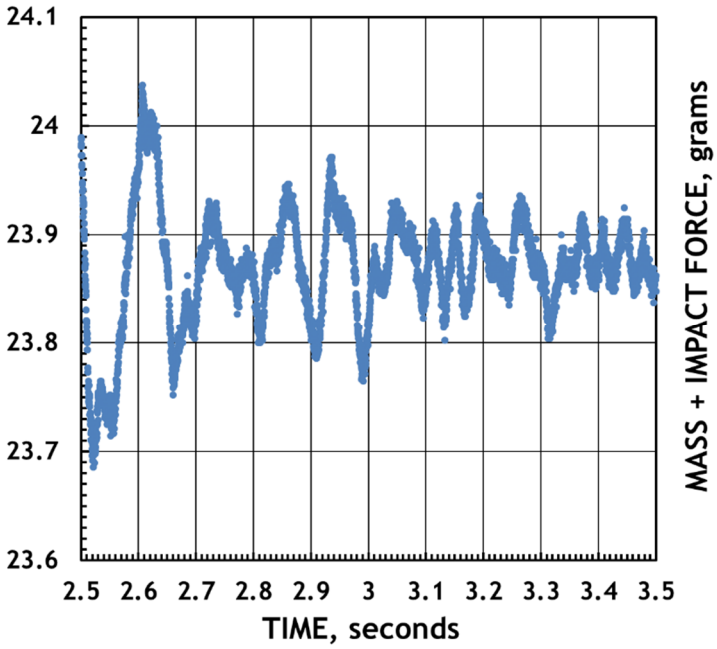

Figure 25. Load Cell Output versus Time for Test SSST025 3 for Sodium Draining from 0.25 inch Stainless Steel Tube with 4.572 mm (0.18 in) Inner Diameter.

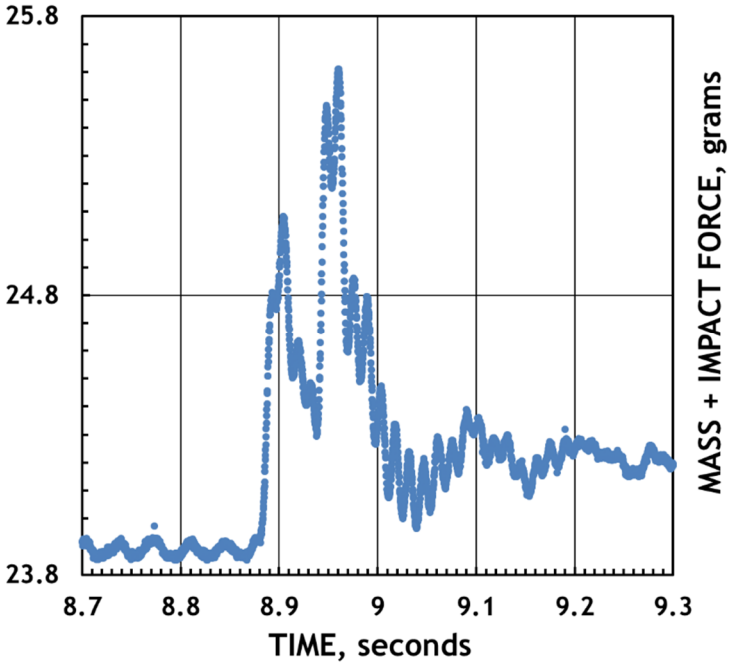

Figure 26. Load Cell Output versus Time for Test SSST025 3 for Sodium Draining from 0.25 inch Stainless Steel Tube with 4.572 mm (0.18 in) Inner Diameter.

An example of the oscillations observed in the load cell output for a selected time interval is shown in Figure **27**. A frequency analysis was performed yielding the spectrum in Figure 28. A peak is evident at 28 Hz. The reason for this oscillation is currently unknown. What is most important is to identify how to eliminate this and similar oscillations in future tests.

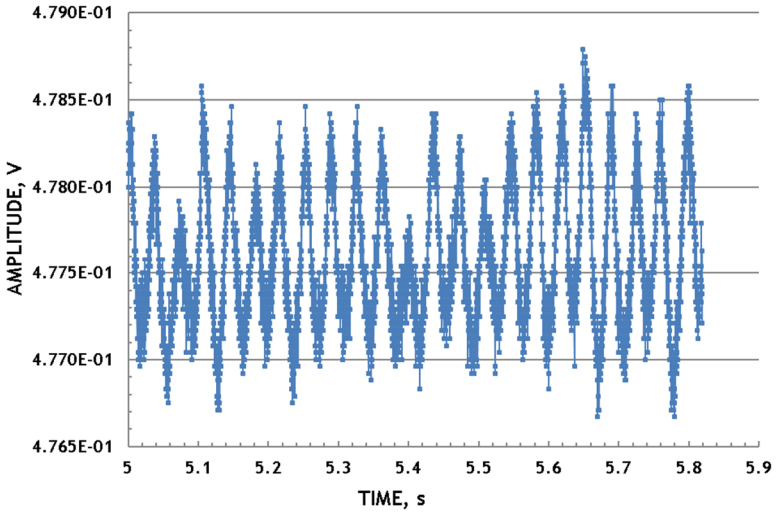

Figure 27. Example of Local Oscillations in Selected Time Interval.

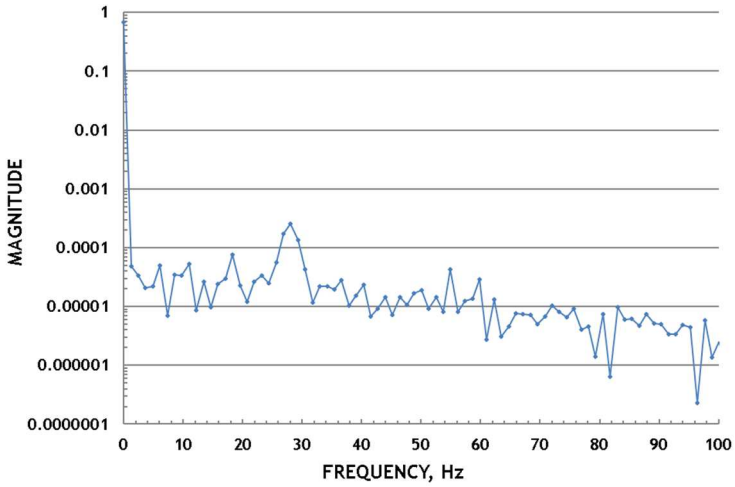

Figure 28. Frequency Analysis of Local Oscillations in Selected Time Interval in Figure 27.

In the third sodium test, data was recorded from the top and bottom pairs of electrodes welded to outer surface of the stainless steel tube 180 degrees apart. The electrodes measure the voltage drop between them that depends upon the effective electrical resistance through both the intervening stainless steel and sodium. The electrical resistivity of sodium is significantly less than that of stainless steel. Thus, the effective electrical resistance increases as the amount of sodium inside the channel in contact with the stainless steel wall decreases.

The electrode data plotted together with the load cell output in Figure 29 through Figure 31is remarkable in what it reveals about the draining phenomena. The raw data shown in Figure 29 is noisy especially for the top electrode rendered in brown. The raw data from the bottom electrode is shown in green. However, by averaging data points, the well behaved purple curve for the top electrode and red curve for the bottom electrode are obtained.

The averaged data clearly show a significant increase in resistance as the slug trailing edge descends through the tube in Figure 31. Thus, timing information about the passage of the slug trailing edge is obtained. The top electrode voltage difference begins to rise at 1.425 s and the bottom voltage difference begins to rise at 1.539 s. Interestingly, the load cell output first starts to rise at 1.45 s. The time difference between the initial increases of the two pairs of electrodes is thus 0.114 s. The distance between the pairs of electrodes is 0.251 m (9.875 in). The mean velocity of the slug trailing edge between the two locations is thus 2.20 m/s.

Following the initial rise from passage of the slug trailing edge, the voltage difference at both pairs of electrodes continues to rise at a slower rate indicating an increase in resistance. This behavior is suggestive of the draining of a sodium film left behind on the tube inner surface that thins with time at each location. In Figure 30, wiggles are seen in both the red and purple curves. These wiggles are suggestive of the descent of waves on the sodium film. However, this wave formation occurs only over a shorter time interval than the thinning of the film. The thinning of the film is nearly complete when the load cell data indicate the discrete draining event at 8.9 seconds.

Thus, the following draining scenario is suggested. Following the rapid slug draining phase, a sodium film is left behind on the tube inner surface. The film slowly drains and collects as a

mass likely near the lower end of the tube. The mass detaches from the tube and is collected in the catch cup. For sodium, the fraction of liquid left behind the slug trailing edge as a film is significantly less than that with water. Thus, there is only sufficient sodium mass for a single discrete draining event later in time versus the multiple rivulets and drops observed in the water tests.

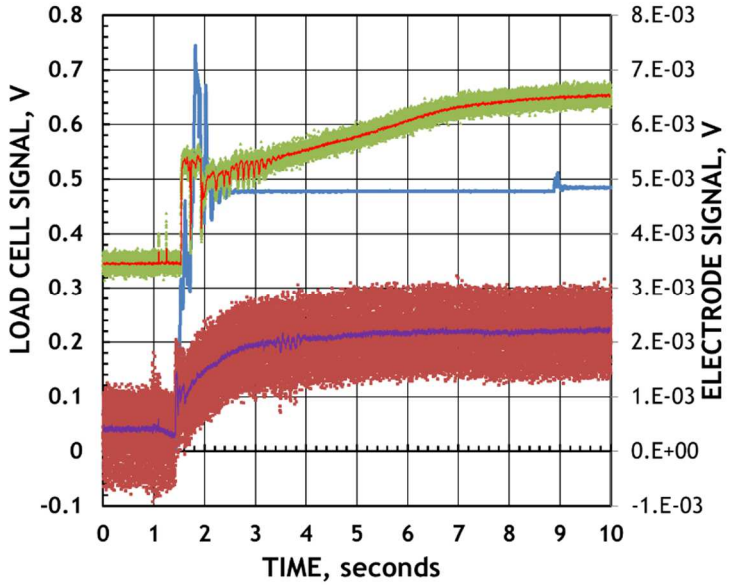

Figure 29. Load Cell Output (Blue) and Electrode Output (Purple Top and Red Bottom) versus Time for Test SSST025 3 for Sodium Draining from 0.25 inch Stainless Steel Tube with 4.572 mm (0.18 in) Inner Diameter.

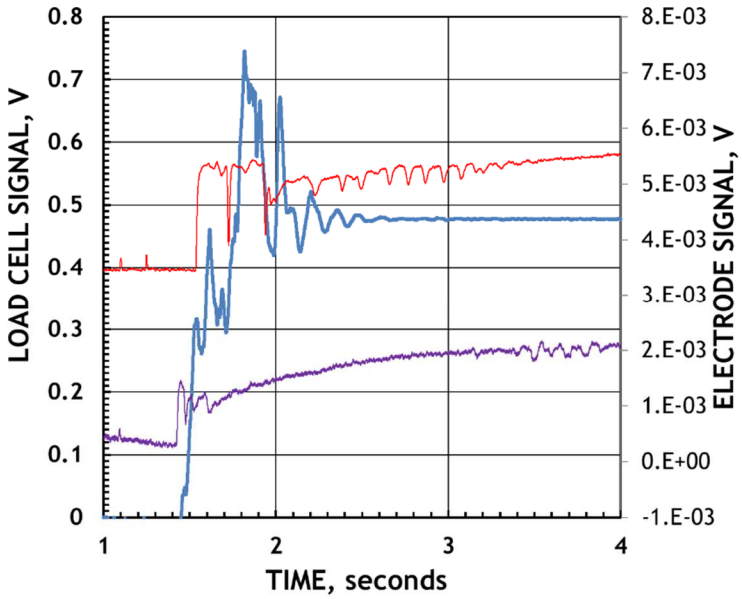

Figure 30. Load Cell Output (Blue) and Electrode Output (Purple Top and Red Bottom) versus Time for Test SSST025 3 for Sodium Draining from 0.25 inch Stainless Steel Tube with 4.572 mm (0.18 in) Inner Diameter.

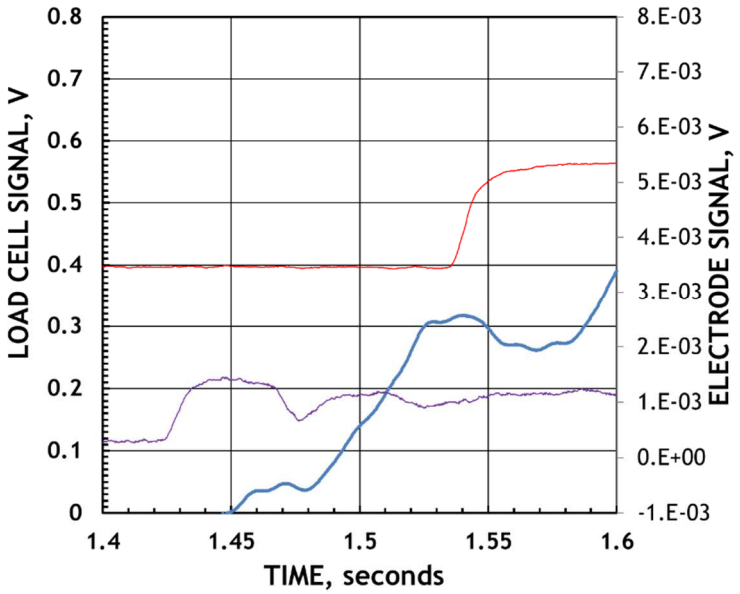

Figure 31. Load Cell Output (Blue) and Electrode Output (Purple Top and Red Bottom) versus Time for Test SSST025 3 for Sodium Draining from 0.25 inch Stainless Steel Tube with 4.572 mm (0.18 in) Inner Diameter.

The methodology applied to the water draining tests to determine mass fractions was applied to the sodium draining tests. It was found to be more difficult to apply because of the nimble response of the load cell dynamic system. In particular, it is more difficult to extrapolate backward to estimate the load cell output reading at the end of the rapid slug draining phase. As mentioned above, there is no clearly discernable linear rate draining phase distinct from a following slow draining phase. The results of applying the methodology are shown below in Table 2. In Table 2, the sodium mass in just the tube in Test SSST025 1 is estimated by subtracting off from the measured sodium total mass the sodium mass estimated between the top of the ball valve and the tube. This mass is estimated by taking the measured water mass of 10.0141 g and multiplying it by the ratio of the sodium density at 175 °C, 908.6 kg/m^3, and the water density at 20 °C, 998.2 kg/m^3. For Tests SSST025 2 and SSST025 3, the sodium mass filling the tube is estimated from the tube inner volume and the sodium density at 225 °C, 897.4 kg/m^3. This provides 6.8295 g. One might consider using the mass inside the tube estimated for the first sodium test. However, it is uncertain that the mass filled the tube given the difficulty in filling the tube in the second and third sodium tests.

As mentioned above, the rapid slug draining time with sodium is significantly less than that with water. In addition, the mass fraction drained during the rapid slug draining phase with sodium is greater than that obtained with water. For Tests SSST025 1, SSST025 2, and SSST025 3, the rapidly drained mass fractions are estimated as 0.9588, 0.9875, and 0.9523, respectively. The mass fractions that drain during the subsequent slow draining phase are 0.0412, 0.0125, and 0.0477, respectively.

The single discrete draining event accounts for most of the mass that drains during the slow draining phase. For the first sodium test, the discrete mass drained is 0.20 g representing a mass

fraction of 0.0356. For the third sodium test, the mass of sodium estimated to drain in the discrete event is equal to the entire mass drained in the slow draining phase, 0.326 g representing a mass fraction of 0.0477. No discrete draining event was observed in the second sodium test. Perhaps this is consistent with the small slowly drained mass faction of only 0.0125.

The existence of a single discrete draining event during the slow draining phase with sodium versus several rivulet and drop draining events with water is thought to simply reflect the fact that significantly lower mass fractions of liquid are left behind inside of the tube following the rapid slug draining phase with sodium relative to water.

These fractions are less than that predicted by the Capillary number correlation for the mass fraction of film left behind on the tube inner wall in horizontal flow which is 0.0902 using the velocity obtained from the rapid slug draining timescale for the first sodium test. Using the mean velocity obtained from the electrode data in the third sodium test, the mass fraction of film left behind on the tube inner wall in horizontal flow is calculated by the Capillary correlation to equal 0.0700.

The data thus shows that sodium drains much more efficiently from a vertical tube than water does.

Table 2. Results for Sodium Draining Tests with Stainless Steel Tubes

Test	SSST025 1	SSST025 2	SSST025 3
Tube ID, mm (in)	4.572 (0.18)	4.572 (0.18)	4.572 (0.18)
Tube Height, m (in)	0.46355 (18.25)	0.46355 (18.25)	0.46355 (18.25)
Rapid Draining Time from Load Cell Plots, s	0.16	0.48	0.54
Rapid Draining Time from Video, s	N/A	N/A	N/A
Total Draining Time, s	4	6	9
Total Mass Drained, g	14.73	24.02	24.226
Mass Drained During Rapid Phase, g	14.5	23.93	23.9
Total Mass Drained from Tube, g	5.617	6.830	6.830
Mass Drained from Tube During Rapid Phase, g	5.385	6.744	6.504
Mass Fraction Drained from Tube During Rapid Phase	0.9588	0.9875	0.9523
Mass Fraction Remaining in Tube After Rapid Phase	0.0412	0.0125	0.0477
Discrete Mass Drained, g	0.20		0.326
Mass Fraction Drained as Discrete Mass	0.0356		0.0477
Mean Velocity Estimated Using Rapid Draining Time from Load Cell Data Plots, m/s	3.65	N/A	N/A
Reynolds Number for Mean Velocity from Rapid Draining Time	35,900	N/A	
Capillary Number for Mean Velocity from Rapid Draining Time	0.00814	N/A	
Mass Fraction Remaining in Tube Predicted Using Horizontal Tube Correlation for Mean Velocity from Rapid Draining Time	0.0902	N/A	
Mean Velocity Estimated Using Time Difference Between Electrode Signals, m/s			2.20
Reynolds Number for Mean Velocity from Electrode Signals			21,600
Capillary Number for Mean Velocity from Electrode Signals			0.00490
Mass Fraction Remaining in Tube Predicted Using Horizontal Tube Correlation for Mean Velocity from Rapid Draining			0.0700

4 Analysis of Sodium Wetting of Stainless Steel

In a SFR, the stainless steel of the heat exchanger will be well wetted by the sodium. Thus, in the sodium draining tests, it is essential that the test section stainless steel is wetted by the sodium. If good wetting were not achieved, then the fraction of liquid mass left behind on the test section inner wall following passage of the slug trailing edge would be expected to be different. The original purpose of the three pairs of voltage probes welded to the outer surface of each stainless steel test section at different elevations was to monitor the extent of wetting as indicated by the effective electrical resistance between opposing probes.

The wetting procedure that was decided upon to ensure that the stainless steel test section is wetted by sodium is to fill the test section with sodium, heat it to 500 °C, and hold it at 500 °C for at least 48 hours. That procedure was shown to be successful by the voltage drops measured by the pairs of electrodes welded to opposite sides of the tube outer surface at three elevations. When the tube is first filled with sodium, there is a contact electrical resistance at the sodium-stainless steel interface due to the initial partial wetting. This limits the fraction of electrical current that flows through the sodium relative to the stainless steel. As wetting proceeds, the contact electrical resistance decreases such that more current flows through the sodium. Because sodium has a significantly lower electrical resistivity relative to stainless steel, the overall resistance and voltage drop decrease as wetting proceeds.

Figure 32 shows the resistances measured between the top pair of electrodes at different times and temperatures. After holding the temperature at 500 °C, the resistance markedly decreases by nearly a factor of five. The × symbol at 500 °C is actually a plot of the measured value over several days. The resistance decreases to a minimum value and remains at that minimum as shown in Figure 33 that plots the measured resistance versus the time in days. It is concluded that wetting was successfully achieved.

Analogous resistance data for the middle and bottom pairs of electrodes is shown in Figure 34 through Figure 37. The resistance values vary from pair to pair. Thus is thought to be due to differences in the voltage probes and the welding to the stainless steel tube. The point is that similar behavior is observed for all three probes indicating that the wetting behavior is universal over the test section.

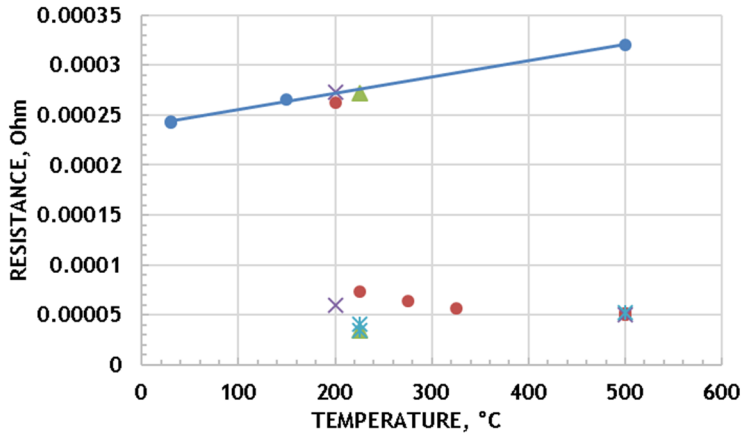

Figure 32. Resistance Between Top Pair of Electrodes. Blue Circles and the Blue Line are the Resistance of the Empty Test Section versus Temperature. Red Circles are the Resistance versus Temperature and Time During the Wetting Procedure. Green Triangles are the Resistance Just Prior To and Following Draining. ×s are the Resistance Just Prior to Filling with Sodium, Immediately After Filling with Sodium, and After One Night with the Temperature Held at 500 °C.

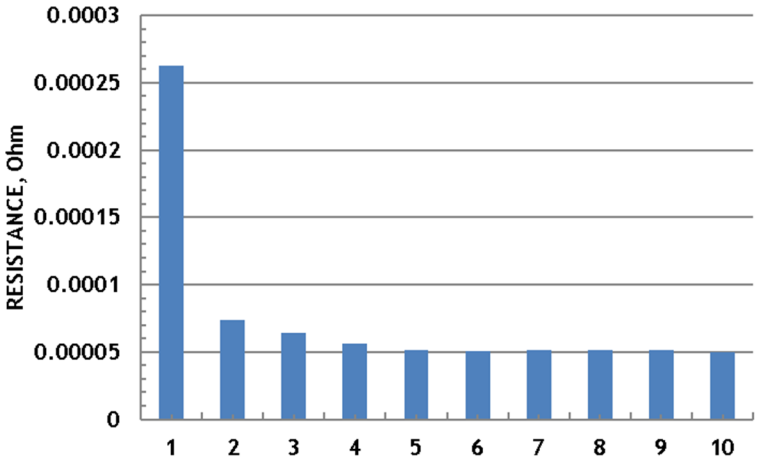

Figure 33. Resistance Between Top Pair of Electrodes at 500 °C versus Time in Days.

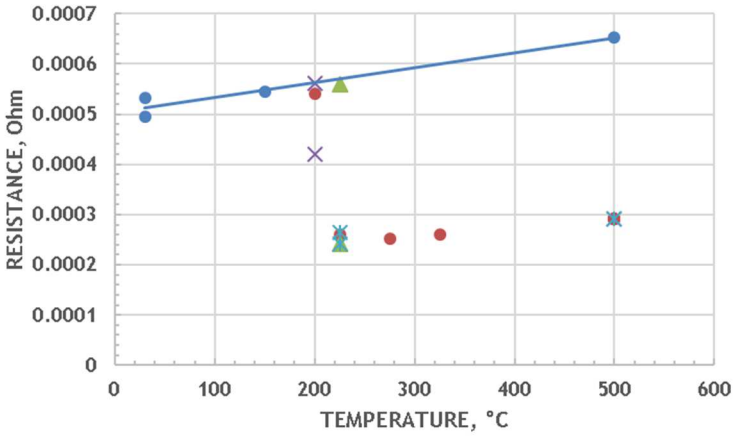

Figure 34. Resistance Between Middle Pair of Electrodes. Blue Circles and the Blue Line are the Resistance of the Empty Test Section versus Temperature. Red Circles are the Resistance versus Temperature and Time During the Wetting Procedure. Green Triangles are the Resistance Just Prior To and Following Draining. ×s are the Resistance Just Prior to Filling with Sodium, Immediately After Filling with Sodium, and After One Night with the Temperature Held at 500 °C.

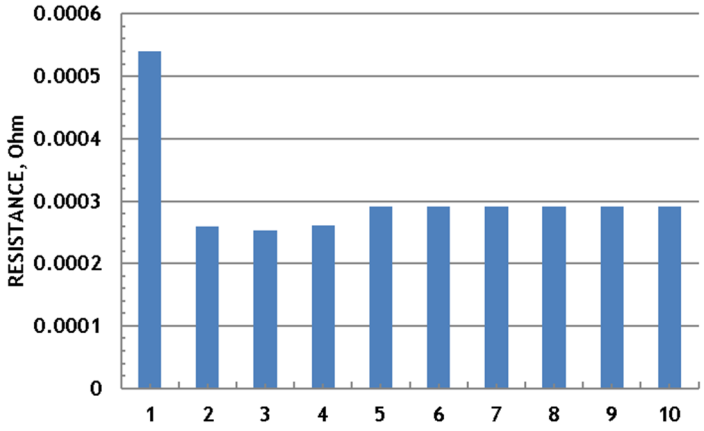

Figure 35. Resistance Between Middle Pair of Electrodes at 500 °C versus Time in Days.

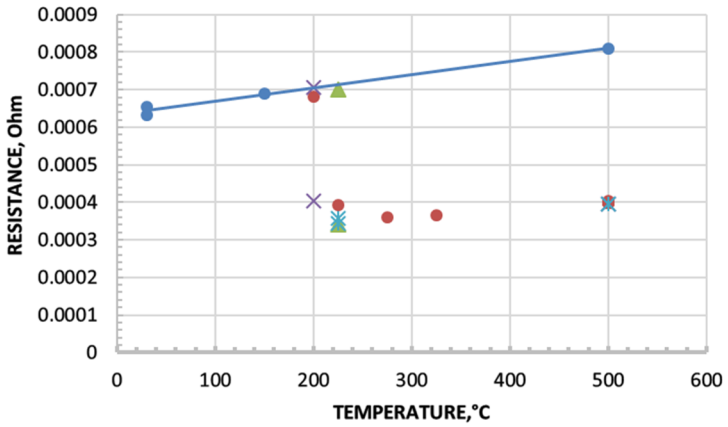

Figure 36. Resistance Between Bottom Pair of Electrodes. Blue Circles and the Blue Line are the Resistance of the Empty Test Section versus Temperature. Red Circles are the Resistance versus Temperature and Time During the Wetting Procedure. Green Triangles are the Resistance Just Prior To and Following Draining. ×s are the Resistance Just Prior to Filling with Sodium, Immediately After Filling with Sodium, and After One Night with the Temperature Held at 500 °C.

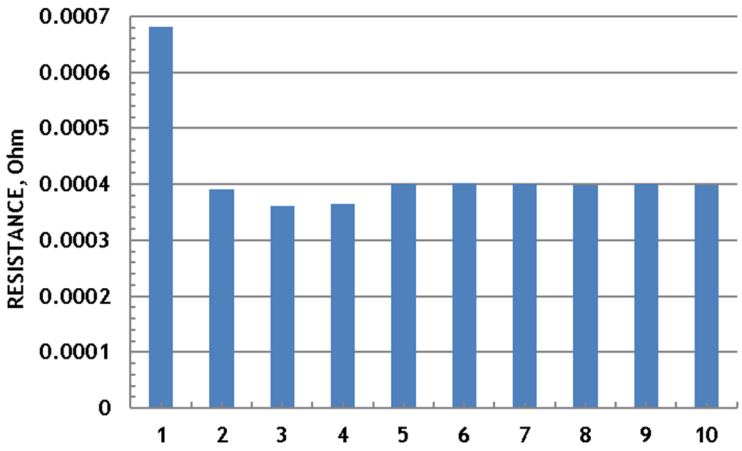

Figure 37. Resistance Between Bottom Pair of Electrodes at 500 °C versus Time in Days.

5 Recommendations and Ideas for Future Tests

Most compact diffusion-bonded heat exchanger designs have channel configurations different than circular channels. The highest priority for future testing is to investigate other channel geometries such as a rectilinear channel and a semicircular channel. The main difference between these other channels and a circular channel is the existence of sharp corners. One can wonder how sharp corners affect the draining of sodium. For a circular channel, a 4.6 mm inner diameter is more than large enough for efficient draining. This suggests investigating rectilinear and semicircular channels with a hydraulic diameter of about 4.6 mm or less. Having the same hydraulic diameter in one or more test sections with different geometries would provide data

about whether draining scales with hydraulic diameter or whether the channel geometry is also important.

The electrode data from pairs of voltage probes welded to the test section outer surface provided remarkable data in the third sodium test. In designing test sections for other geometries, the amount of steel needs to be limited such that the voltage drop at each pair of voltage probes is sensitive to the draining of sodium and thinning of sodium left behind as a film upon the channel inner surface.

The draining and thinning of a sodium film left behind the slug trailing edge is inferred from the electrical resistance data measured with the voltage probes. It would be interesting to estimate the initial sodium film thickness with modeling for the effective resistance as a function of the assumed sodium film thickness and compare that thickness with that implied by the mass fraction of sodium left behind obtained from the load cell data.

An improvement to the facility would be to replace the 10.16 mm inner diameter tube segment below the test section with one specific to each test section having the same geometry and inner dimensions as the test section.

Performing sodium draining tests with smaller diameters is of interest. Performing sodium draining tests with greater diameters is of less interest because if a smaller diameter is adequate, then there is far less incentive to go to a larger diameter for a sodium channel when designing a compact diffusion-bonded heat exchanger. Varying the channel diameter upward is more of interest in understanding how the phenomena scale with diameter.

The nature of the discrete mass draining events with sodium is inferred from the voltage probe resistance data in the third sodium test. The draining events cannot be visualized through the wall of the stainless steel tube. Such single draining events were not observed in any of the water draining tests. Thus, using water as a simulant with a glass or plastic tube is not a viable approach.

When sodium draining tests are resumed and a new test section is used for the first time, the first sodium draining test(s) should be non-wetting. By this it is meant that the sodium is pushed up into the stainless steel test section but the sodium and stainless steel are not elevated in temperature purposely to promote wetting. Thus, they are not raised in temperature to 500 °C and held at that temperature for 48 hours. The purpose of non-wetting tests is to compare the draining behavior with that obtained after wetting has been achieved. For a perfectly non-wetting fluid, no fluid mass should be left behind as a film upon the channel wall. The liquid slug should contract away from the wall, perhaps break up into multiple slugs, and fall through the test section. If a difference between a non-wetting and a wetted test under similar conditions of sodium mass is observed, that is further evidence that wetting was successfully achieved. A potential complication with sodium is that when sodium and stainless steel are initially brought into contact at temperatures below 250 °C, there is some partial wetting. The contact angle is 140 degrees [6]; non-wetting is a contact angle of 180 degrees. Still, 140 degrees is close to non-wetting and the difference in results between non-wetting and wetted tests is still of great interest.

For future sodium tests, it is thought that it will be beneficial to hang weights from the brim of the collection cup to increase the mass atop of the load cell. This should reduce the accelerations and thereby reduce the magnitude of the load cell dynamic system oscillations and overshoots.

The reason for the many oscillations observed in the third sodium test is unknown. This needs to be understood and the unwanted oscillations eliminated before more tests are performed.

There is a need to experimentally investigate smaller channel diameters near that for which liquid lenses are predicted to form and bridge the channel such that liquid may remain inside of the channel and not drain. The critical diameter for both water and sodium is predicted with a correlation to be 2.2 mm. However, performing draining tests with a channel as small as 2 mm is challenging as the mass involved is extremely small. In particular, for a 0.46 m high 2 mm inner diameter tube, the liquid mass drained is less than 1.5 g.

6 Summary

Sodium and water both drain efficiently from a vertical stainless steel tube with an inner diameter of 4.6 mm. This is an important and good result for the design of compact diffusion-bonded heat exchanger sodium channels. Sodium drains more efficiently than water. This is also an important and good result for the design of compact diffusion-bonded heat exchanger sodium channels. The draining phenomena observed with sodium and water are significantly different. The draining of water involves an initial rapid slug draining phase followed by a linear rate draining phase followed by a slow draining phase involving draining of rivulets and drops. This behavior has previously been reported in the literature for viscous fluids. The draining of sodium involves an initial rapid slug draining phase but no discernable linear rate draining phase. There is a subsequent slow draining phase. However, unlike the slow draining phase with water that involves a number of rivulets and drops, the slow draining phase with sodium in two out of three sodium tests mainly involves a single discrete event in which a mass of sodium drains from the tube. This single discrete draining event encompasses most of the sodium mass remaining inside of the tube following the rapid slug draining phase. The existence of a single discrete draining event during the slow draining phase with sodium versus several rivulet and drop draining events with water is thought to simply reflect the fact that significantly lower mass fractions of liquid are left behind inside of the tube following the rapid slug draining phase with sodium relative to water. For the sodium tests, the progress of wetting of the stainless steel by sodium was monitored by means of the voltage drop across the tube outer diameter measured by pairs of opposing electrodes welded to the tube outer surface at three different elevations. The electrode data remarkably reveals phenomena during the sodium draining. The downward passage of the sodium slug trailing edge past each electrode was observed from which a mean slug trailing edge velocity could be determined. The subsequent slower increase in voltage drop suggests draining and thinning of a sodium film left behind upon the tube inner surface; wiggles in the voltage drop data are suggestive of the descent of waves on the film. It is thought that the draining sodium film collects as a mass likely near the lower end of the tube and detaches corresponding to the single discrete draining event observed in the load cell data. The minimum circular channel inner diameter for the draining of water and sodium without the formation of lenses that bridge the channel and may remain inside of the tube without draining is predicted with a correlation to be

2.2 mm. The highest priority for future sodium draining testing is to investigate other channel geometries such as a rectilinear channel or a semicircular channel.

Acknowledgements

Argonne National Laboratory's work was supported by the U. S. Department of Energy Nuclear Technology Research and Development Program under Prime Contract No. DE-AC02-06CH11357 between the U.S. Department of Energy and UChicago Argonne, LLC. The work presented here was carried out under the Fast Reactors area of the Program. The authors are grateful to Chris Grandy (Argonne/Nuclear Science and Engineering), the Technical Area Lead, Bob Hill (Argonne/Nuclear Science and Engineering), the National Technical Director, as well as Alice Caponiti and Tom Sowinski (U.S. DOE), Headquarters Program Managers for the Project. The authors are also grateful to Claude Reed (Argonne/Nuclear Science and Engineering) for his Environment Safety and Health guidance.

References

1. D. B. Chojnowski, E. Boron, J. J. Sienicki, Y. Momozaki, and C. B. Reed, "FY 2017 Progress Report on the Argonne Sodium Draining and Refilling Experiments," ANL-ART-126, Argonne National Laboratory, Nuclear Engineering Division, September 15, 2017.

2. A. Ali, A. Underwood, Y.-R. Lee, and D. I. Wilson, "Self-Drainage of Viscous Liquids in Vertical and Inclined Pipes," Food and Bioproducts Processing, Vol. 99, pp. 38-50, 2016.

3. F. Fairbrother and A. E. Stubbs, "Studies in Electro-endosmosis. Part VI. The "Bubble-tube Method of Measurement," Journal of the Chemical Society (Resumed), 1935, Paper 119, pp. 527-529.

4. G. I. Taylor, "Deposition of a Viscous Fluid on the Wall of a Tube," Fluid Mechanics, Vol. 10, pp. 161-165, 1961.

5. O. E. Jensen, "Draining Collars and Lenses in Liquid-Lined Vertical Tubes," Journal of Colloid and Interface Science, Vol. 221, pp. 38-49, 2000.

6. E. N. Hodkin, Mrs. D. A. Mortimer, and M. Nicholas, "The Wetting of Some Ferrous Materials by Sodium," Liquid Alkali Metals, Proceedings of the International Conference Organized by the British Nuclear Energy Society, Held at Nottingham University on 4-6 April 1973, The British Nuclear Energy Society, London, 1973.

.

Nuclear Science and Engineering Division
Argonne National Laboratory
9700 South Cass Avenue, Bldg. 208
Argonne, IL 60439

www.anl.gov